Loss of function mutation of the Slc38a3 glutamine transporter reveals its critical role for amino acid metabolism in the liver, brain, and kidney

Chan, Kessara ; Busque, Stephanie M ; Sailer, Manuela ; Stoeger, Claudia ; Bröer, Stefan ; Daniel, Hannelore ; Rubio-Aliaga, Isabel ; Wagner, Carsten A

Abstract: Glutamine, the most abundant amino acid in mammals, is critical for cell and organ functions. Its metabolism depends on the ability of cells to take up or release glutamine by transporters located in the plasma membrane. Several solute carrier (SLC) families transport glutamine, but the SLC38 family has been thought to be mostly responsible for glutamine transport. We demonstrate that despite the large number of glutamine transporters, the loss of Snat3/Slc38a3 glutamine transporter has a major impact on the function of organs expressing it. Snat3 mutant mice were generated by N-ethyl-N-nitrosurea (ENU) mutagenesis and showed stunted growth, altered amino acid levels, hypoglycemia, and died around 20 days after birth. Hepatic concentrations of glutamine, glutamate, leucine, phenylalanine, and tryptophan were highly reduced paralleled by downregulation of the mTOR pathway possibly linking reduced amino acid availability to impaired growth and glucose homeostasis. Snat3-deficient mice had altered urea levels paralleled by dysregulation of the urea cycle, gluconeogenesis, and glutamine synthesis. Mice were ataxic with higher glutamine but reduced glutamate and gamma-aminobutyric acid (GABA) levels in brain consistent with a major role of Snat3 in the glutamine-glutamate cycle. Renal ammonium excretion was lower, and the expression of enzymes and amino acid transporters involved in ammoniagenesis were altered. Thus, SNAT3 is a glutamine transporter required for amino acid homeostasis and determines critical functions in various organs. Despite the large number of glutamine transporters, loss of Snat3 cannot be compensated, suggesting that this transporter is a major route of glutamine transport in the liver, brain, and kidney.

DOI: https://doi.org/10.1007/s00424-015-1742-0

Loss of function mutation of the Slc38a3 glutamine transporter reveals its critical role for amino acid metabolism in liver, brain, and kidney

Kessara Chan[1,*], Stephanie M. Busque[1], Manuela Sailer[2], Claudia Stoeger[3], Stefan Bröer[4], Hannelore Daniel[2] , Isabel Rubio-Aliaga[1,2#], Carsten A. Wagner[1#]

From the [1]Institute of Physiology and Zurich Center for Integrative Human Physiology (ZIHP), University of Zurich, Zurich, Switzerland, [2]ZIEL Research Center of Nutrition and Food Sciences, Department of Biochemistry, Technische Universität München, Freising, Germany, [3]Ingenium, Munich, Germany, [4]Research School of Biology, Australian National University, Canberra, Australia

#To whom correspondence should be addressed: Carsten A. Wagner or Isabel Rubio-Aliaga, Institute of Physiology, University of Zurich, Winterthurerstrasse 190, CH-8057 Zurich, Switzerland, Tel.: +41(0)44 635 50 23, Fax: +41 (0)44 635 68 14, email: wagnerca@access.uzh.ch or isabel.rubioaliaga@uzh.ch

*Current address: Institute of Molecular Health Sciences, ETH Zurich, Zurich, Switzerland

Running title: Central role of Snat3 in glutamine homeostasis

Keywords: amino acid transport, glutamine metabolism, mouse model, ammoniagenesis, mTOR pathway

ABSTRACT

Glutamine, the most abundant amino acid in mammals, is critical for cell and organ functions. Its metabolism depends on the ability of cells to take up or release glutamine by transporters located in the plasma membrane. Several solute carrier (SLC) families transport glutamine, but the SLC38 family has been thought to be mostly responsible for glutamine transport. We demonstrate that despite the large number of glutamine transporters, loss of the Snat3/Slc38a3 glutamine transporter has a major impact on the function of organs expressing it. *Snat3* mutant mice were generated by N-ethyl-N-nitrosurea (ENU) mutagenesis and showed stunted growth, altered amino acid levels, hypoglycemia, and died around 20 days after birth. Hepatic concentrations of glutamine, glutamate, leucine, phenylalanine, and tryptophan were highly reduced paralleled by downregulation of the mTOR pathway possibly linking reduced amino acid availability to impaired growth and glucose homeostasis. *Snat3* deficient mice had altered urea levels paralleled by dysregulation of the urea cycle, gluconeogenesis, and glutamine synthesis. Mice were ataxic with higher glutamine but reduced glutamate and GABA levels in brain consistent with a major role of Snat3 in the glutamine-glutamate cycle. Renal ammonium excretion was lower and expression of enzymes and amino acid transporters involved in ammoniagenesis were altered. Thus, SNAT3 is a glutamine transporter required for amino acid homeostasis and determines critical functions in various organs. Despite the large number of glutamine transporters, loss of Snat3 cannot be compensated suggesting that this transporter is a major route of glutamine transport in liver, brain, and kidney.

INTRODUCTION

Glutamine is the most abundant amino acid in the human body and is involved in more physiological processes than any other amino acid [1-3]. Glutamine serves as a precursor of purines, pyrimidines, glycogen, glucose, and in protein synthesis [4] and is involved in a myriad of other metabolic processes. It is also a major regulator of key physiologic processes such as hepatic and renal gluconeogenesis, the glutamate/GABA-glutamine cycle in the central nervous system (CNS) [5], hepatic ammonia detoxification [6], and in renal response to acidosis [7]. Furthermore, glutamine is the major oxidative fuel for rapidly replicating cells such as enterocytes and cells of the immune system, providing ATP for intracellular protein turnover, nutrient transport through the plasma membrane, cell growth and migration as well as the maintenance of cell integrity [1, 8]. Finally, glutamine is also a key intermediate in interorgan nitrogen and carbon transport [9-10]. The transport of glutamine across cell membranes is mediated by several amino acid carriers with different specificity for glutamine and other neutral amino acids. To date, at least 4 distinct SLC transporter families have been implicated in glutamine transport, the SLC1 family of glutamate and glutamine transporters, the SLC3-SLC7 heterodimeric family, the SLC6 family of neurotransmitter and neutral amino acid transporters, and the SLC38 family of glutamine transporters [11-12]. The SLC38 family has at least two major subgroups, the system A transporter of Na^+-coupled transporters including SNAT1 (SLC38A1), SNAT2 (SLC38A2), and SNAT4 (SLC38A4) and the system N transporter family of Na^+- and H^+-coupled transporters SNAT3 (SLC38A3), SNAT5 (SLC38A5), and SNAT7 (SLC38A7) [13]. Whereas system A transporters have a wider substrate spectrum including glutamine, alanine, asparagine, cysteine, serine, methionine, proline, glycine, and histidine, the specificity of system N transporters is

narrow transporting only glutamine, histidine, asparagine, and serine [12]. These system N amino acid transporters mediate the uptake of 1 glutamine molecule with the net uptake of 1 Na^+ in exchange of a proton. The other members of the SLC38 family, the system A transporters (SNAT1, SNAT2, SNAT4) are not able for counter-transport of protons [13-16]. SNAT3 is highly abundant in liver, kidney, and brain, and expression has also been reported for adipose tissue, pancreas, skeletal muscle, and eye. In kidney, SNAT3 is mainly localized to the proximal tubule, in liver to both perivenous and periportal hepatocytes, and in brain mostly in astrocytes and endothelial cells of the blood-brain-barrier [17-21]. In the brain, SNAT3 and SNAT5 have been hypothesized to be responsible for the efflux of glutamine from astrocytes which is a crucial step in the recycling of glutamate and GABA neurotransmitters between astrocytes and neurons [5, 22]. In the liver, SNAT3 is likely to be a candidate for both periportal uptake and perivenous efflux of glutamine, which is essential for the detoxification of ammonia delivered via the portal blood and excreted as urea [6, 21]. Furthermore, SNAT3 mRNA and protein expression in the kidney is increased in response to metabolic acidosis possibly providing glutamine for ammoniagenesis in the proximal tubule cell [18, 20, 23-24]. Plasma glutamine levels decrease substantially during metabolic acidosis [25] and glutamine flow is redirected from the splanchnic bed to the kidney with SNAT3 proposed to deliver glutamine for renal ammoniagenesis.

To date, all studies addressing the function and regulation of SLC38 amino acid transporters have used either heterologous expression systems or cell culture models. The biological relevance of these transporters, however, has not been examined in any *in-vivo* model to the best of our knowledge. Here we demonstrate

that SNAT3 plays a critical role in glutamine transport and metabolism by characterizing a mouse model deficient of Slc38a3.

MATERIALS AND METHODS

Animals. Snat3 mutant mice (Q263X, Hybrid C3H-C57BL/6J) were generated by Ingenium Pharmaceuticals AG (Martinsried, Germany) using ENU-mutagenesis. The mutation causes a premature stop codon at amino acid position 263 deleting the second half of the protein (Fig. 1B). Animals were maintained at 22 ± 2°C and a 12:12 h light/dark cycle with access to tap water and standard rodent diet ad libitum (Provimi KLIBA, Kaiseragust, Switzerland). Mice were continuously backcrossed to C57BL6/J and animals from the 6 to 10th generation were used for this study. For all experiments littermates were used from heterozygous breeding. Analysis of the offspring from heterozygous mating suggested that the ratio of genotypes obtained followed almost a Mendelian inheritance (wildtype (WT) 15%, *Snat3*$^{+/-}$ 56%, *Snat3*$^{-/-}$ 29%; n = 52 pups analyzed). All animal procedures were carried out according to the Swiss Animal Welfare laws and approved by the local veterinary authority (Kantonales Veterinäramt Zurich).

mRNA analysis by semi-quantitative real time PCR. Snap-frozen tissue was homogenized in 1 ml RLT-buffer (Qiagen, Netherland) supplemented with 2- using RNeasy Mini Kit (Qiagen, Netherland) following the manufacturer's instructions. Quality, purity and concentration of the isolated RNA were assessed susing the ND-1000 spectrophotometer (NanoDrop technologies, USA).

Each RNA sample was diluted to 100 ng/µl and 3 µl was used as a template for reverse transcription using the TaqMan Reverse Transcription Kit (Applied Biosystems, USA). Reverse transcription was performed with the Biometra

TGradient thermocycler with termocycling conditions set at 25°C for 10 min, 48°C for 30 min, and 95°C for 5 min. Semi-quantitative real-time (RT-qPCR) was performed on the ABI PRISM 7700 Sequence Detection System (Applied Biosystem, USA). Thermocycling conditions were as follows: 50°C for 2 min, 95°C for 10 min, and 95°C for 15 s (40 cycles). Primers and probes for all genes were designed using Primer 3 Software developed at Whitehead Institute and Howard Hughes Medical Institute and synthesized at Microsynth (Microsynth, Balgach,Switzerland). Probes were labeled with the reporter dye FAM at the 5' end and the quencher dye TAMRA at the 3' end (Microsynth, Balgach, Switzerland). Reactions were run in triplicate, including a negative control (without Multiscribe reverse transcription enzyme). The gene expression was calculated in relation to hypoxanthine guanine phosphoribosyl transferase (HPRT). Relative expression were calculated as $2^{[(Ct(HPRT)-Ct(test\ gene)]}$. Primers and probes are listed in Supplementary Table 1.

Antibodies. The primary antibodies used were mouse monoclonal anti-ß-actin (42 kDa; Sigma-Aldrich, Saint-Louis, MO, USA; diluted 1:5000), mouse monoclonal anti-tubuline antibody (50 kDa; Sigma-Aldrich, Saint-Louis, MO, USA; diluted 1:20000), rabbit polyclonal anti-PEPCK antibody (63 kDa; Cayman Chemicals, Ann Arbor, MI, USA; diluted 1:1000), rabbit polyclonal anti-PDG antibody (66 and 68 kDa; a kind gift from N. Curthoys, Colorado State University, Fort Collins, CO, USA [26]; diluted 1:5000), rabbit polyclonal anti-GLS2 antibody (70 kDa; ProSci, Poway, CA, USA; diluted 1:2000), rabbit monoclonal anti-Glu1 (45 kDa; BD Transduction Laboratories, San Jose, CA, USA; diluted 1:5000), rabbit polyclonal anti EAAT2 antibody (53 kDa; Cell Signaling Technology, Boston, MA, USA; diluted 1:2000), rabbit polyclonal anti-EAAT3 antibody (Alpha Diagnostic International, San Antonio, TX, USA; diluted

1:2000), polyclonal anti- total-S6K antibody (70 kDa, Cell Signaling Technology, Boston, MA, USA; diluted 1:5000), rabbit polyclonal anti-LAT1 (39 kDa; kind gift of N. Thompson, Brown University, Providence, RI, USA [27]; diluted 1:1000) and anti-LAT2 (39 kDa; a kind gift from F. Verrey, Zurich University,, Switzerland, [28] ; diluted 1:1000), rabbit polyclonal anti-phospho-p70 SK6 antibody (70 kDa, Cell Signaling Technology, Boston, MA, USA ; diluted 1:5000), rabbit polyclonal anti-total mTOR antibody (289 kDa; Cell Signaling Technology, Boston, MA, USA; diluted 1:5000) and rabbit polyclonal anti-phospho-mTOR antibody (289 kDa; Cell Signaling Technology, Boston, MA, USA; diluted 1:2000). Rabbit polyclonal anti-SNAT1 (55 kDa; kindly provided by F. Verrey, University of Zurich, Zurich, ZH, Switzerland [19]; diluted 1:1000), rabbit polyclonal anti-SNAT3 (55 kDa; kindly provided by F. Verrey, University of Zurich, Zurich, ZH, Switzerland [20]; diluted 1:500). Secondary antibodies used were horseradish peroxidase-conjugated donkey anti rabbit or anti mouse (GE Healthcare, Little Chalfont, Buckinghamshire, United Kingdom; diluted 1:10000) and goat alkaline phosphatase-conjugated anti-rabbit (Promega, Madison, WI, USA, diluted 1:5000), Alexa 593 anti-rabbit antibody (Invitrogen, Carlsbad, CA, USA); diluted 1:1000) and Alexa 488 donkey anti-goat antibody (Invitrogen Carlsbad, CA, USA; diluted 1:3000).

Protein extraction and immunoblotting. Kidneys, liver and brain were removed from 14 days old mice and rapidly frozen in liquid nitrogen. Total membrane and cytosolic proteins were prepared using a K-HEPES buffer (200 mM mannitol, 80 mM K-HEPES, 41 mM KOH, pH 7.5) containing protease inhibitors (PMSF, K-EDTA, and leupeptin). The different organs were homogenized using a Rotor-stator homogenizer. Kidneys and liver homogenates were subsequently centrifuged for 20

min at 2,000 rpm at 4°C, whereas the brain was centrifuged for 30 min at 3,500 rpm at 4°C due to the high content of fat. The supernatant was ultra-centrifuged (Sorvall, Thermo Fisher Scientific, Waltham, MA, USA) for 1h at 41,000 rpm at 4°C. The resulting supernatant containing the cytosolic proteins was removed and the pellet resuspended in K-HEPES buffer and sonicated briefly to homogenize the proteins solution. Total protein concentration was measured using the Bio-Rad DC protein assay (Bio-rad, Hercules, CA, USA). Fifty µg of crude membrane proteins were solubilized in 2X Laemmli sample buffer and SDS page was performed on either 6% or 10% polyacrylamide gels. Proteins were transferred to polyvinylidene difluoride (PVDF) membranes (Immobilon-P, Milipore, Billerica, MA USA). After blocking with 5% milk powder in Tris -buffered saline/01% Tween-20 for 1h, blots were incubated with primary antibodies either at room temperature for 2h or overnight at 4°C. Membranes were then washed three times, blocked for 1h in 5% milk TBS tween, and incubated for 1h at room temperature with secondary antibodies. Membranes were treated with alkaline phosphatase or horseradish peroxidase-conjugated developing solution and exposed to the las4000 chemiluminescence detection system (Fujifilm, Tokyo, Japan). Specific bands on PVDF membranes were quantified using AIDA Image Analyser. Eventually membranes were stripped and reprobed with other antibodies.

Immunochemistry. Anesthetized mice were perfused through the left cardiac ventricle with a phosphate-buffered saline (PBS, pH 7.4), followed by a 1 % paraformaldehyde/ 2.5 glutaraldehyde fixative solution. Kidneys, liver and brain were then harvested and left in the fixative solution overnight. Organs were embedded in O.C.T. Compound (Tissue-Tek, Sakura Finetek, Alphen aan den Rijn, Netherlands)

and store at -80C°. For staining, 3-µm-thick tissue sections were prepared using a vibrating microtome VT1000S (Leica, Aarau, AG, Switzerland) and mounted on polylysine-coated glass slides (Kindler, Freiburg, BW, Germany). Sections were treated in SDS for 5 min, blocked for 15 minutes with bovine serum albumin), and incubated with primary antibodies overnight at 4C°. Sections were washed three times with PBS/high salt (0.3 M NaCl) and once with PBS, then incubated with Alexa labeled secondary antibodies and 4',6-diamidino-2-phenylindole (DAPI, Invitrogen Carlsbad, CA, USA; diluted 1:1000) to mark cell nuclei. After washing sections twice with PBS/high salt and once with PBS, sections were mounted in an aqueous mounting medium (Glycergel, Dako, Glostrup, Denmark). Sections were viewed on a Leica 5500B microscope (Leica, Aarau, AG, Switzerland) and pictures processed using Adobe photoshop.

Amino acids measurements in plasma and organs. For quantification of amino acids a LC-MS/MS based method with aTRAQ® labeling (Reagent Kit, ABSciex, Foster City, USA) was employed [29]. For analysis of tissue amino acids (brain, liver, kidney) small pieces of tissues were homogenized in liquid nitrogen. 100 mg of homogenized tissue were dissolved in 150 µl MeOH/H_2O (50/50, v/v), vortexed, and centrifuged. Sample preparation was done according to the manufacturer's instructions using 40 µl of the supernatant of the tissue homogenates or 40 µl plasma. Tissue amino acid concentrations were standardized with protein concentrations determined via Bradford assay (Bio-Rad Laboratories GmbH, Germany).

Plasma glucose, insulin and ammonium measurements. Blood glucose measurements were carried out using ACCU-CHEK Aviva Plus system (Roche, Basel, BS, Switzerland). Mice were anesthetized and one drop of blood from the tail vein was collected for glucose measurements. Plasma insulin measurements were performed using the ultra-sensitive mouse insulin ELISA kit according to the manufacturer's instructions (Crystal Chem, Downers Grove, IL, USA). Similarly, plasma ammonium measurements were performed using the Sigma ammonium assay kit according to the manufacturer's instructions (Sigma-aldrich, Saint-Louis, MO, USA).

Induction of metabolic acidosis. Wildtype *and* heterozygous *Snat3* mutant mice were placed in metabolic cages for 4 days and urine collected under mineral oil on the last day for 24 hrs. One group of wildtype and mutant mice received only standard rodent chow and tap water ad libitum. A second group of mice received for the last two days 0.28 M NH_4Cl in drinking water to induce metabolic acidosis as described previously [30]. Animals were sacrificed and their kidneys harvested and immediately frozen. Urinary pH was measured using a pH microelectrode (691 pH-meters, Metronohm, Herisau, AR, Switzerland). Urinary creatinine was measured according to the Jaffe method [31]. Urinary ammonium was measured by the Berthelot method [32].

Statistical analysis and graphs. Results are expressed as mean ± SEM. All data were tested for significance using the one-way ANOVA and Tukey post-test or unpaired student's t-test where appropriate. Graps were generated using Prism GraphPad (La Jolla, CA, USA).

RESULTS

Snat3 mutant mice die in the late weaning stage

Snat3 mRNA expression was first studied in wildtype mice. Real-time PCR confirmed a significant expression of *Snat3* in brain, kidneys, eyes, skeletal muscles and the highest expression in liver (Fig. 1A). However, since 14 days old mice could not provide enough material for experiments on muscles and eyes, further studies were performed only on brain, kidneys, and liver. Mutant mice were obtained from screening a library of sperm generated using ENU mutagenesis [33]. Deletion of *Snat3/Slc38a3* in mice was lethal; homozygous mutant mice (*Snat3*$^{-/-}$) died between 18 and 20 days after birth whereas no increased lethality was observed for heterozygous mice (*Snat3*$^{+/-}$). Homozygous mutant mice were easily distinguishable by their small size (Fig. 1C), lower body weight at postnatal day 14 (WT: 8.1 ± 0.2 g; *Snat3*$^{+/-}$*:* 8.2 ± 0.1g, and *Snat3*$^{-/-}$*:* 5.1 ± 0.3 g; 7-33 animals/group, $p < 0.001$ for *Snat3*$^{-/-}$ vs. WT or *Snat3*$^{+/-}$) and a form of ataxia. In homozygous mutant mice, lower signals of *Snat3* mRNA expression was detected by real-time PCR in the brain, liver and kidney (Fig. 1D-F). Western Blot analysis did not detect any Snat3 protein expression in tissue extracts of brain, liver and kidney from *Snat3*$^{-/-}$ mice, demonstrating that the mutation leads to the ablation of Snat3 expression (Fig. 1G-I). Interestingly, heterozygote mice (*Snat3*$^{+/-}$) showed intermediate expression levels of *Snat3* mRNA and protein. Furthermore, kidney sections from *Snat3*$^{-/-}$ mice showed no staining for the transporter in the proximal tubule, hence confirming the deletion of the protein (Fig. 1J).

Snat3 deletion causes hypoglycemia and altered amino acids levels in mutant mice

Because SNAT3 is an amino acid transporter, we expected that amino acid concentrations in the blood of mutant mice might be altered. Indeed, the plasma concentration of histidine (WT: 120.99 ± 12.09 vs. *Snat3*$^{-/-}$: 469.36 ± 39.54 mmol/L), threonine (WT: 231.45 ± 26.81 vs. *Snat3*$^{-/-}$: 293.92 ± 14.45 mmol/L), leucine (WT: 133.36 ± 7.79 vs. *Snat3*$^{-/-}$: 191.95 ± 26.84 mmol/L), cysteine (WT: 3.05 ± 0.04 vs. *Snat3*$^{-/-}$: 3.31 ± 0.20 mmol/L), and carnosine (WT: 9.88 ± 0.78 vs. *Snat3*$^{-/-}$: 20.50 ± 3.03 mmol/L) was significantly higher in homozygous mutant mice whereas the concentration of tyrosine (WT: 150.32 ± 13.41 vs. *Snat3*$^{-/-}$: 95.08 ± 9.47 mmol/L), alanine (WT: 778.82 ± 45.07 vs. *Snat3*$^{-/-}$: 541.17 ± 26.83 mmol/L), and tryptophan (WT: 87.70 ± 4.43 vs. *Snat3*$^{-/-}$: 67.30 ± 6.01 mmol/L) was significantly lower (Supplementary Table 2).

Next, we measured amino acid concentrations in liver to determine if changes in plasma amino acid concentrations would also correlate with changes in amino acid availability in this organ (Supplementary Table 3). Alanine (WT: 57.52 ± 9.72 vs. *Snat3*$^{-/-}$: 28.99 ± 4.99 µmol.L^{-1}/µg.µL^{-1}), glutamine (WT: 84.02 ± 10.11 vs. *Snat3*$^{-/-}$: 36.73 ± 7.63 µmol.L^{-1}/µg.µL^{-1}), glutamate (WT: 67.40 ± 6.96 vs. *Snat3*$^{-/-}$: 42.88 ± 11.46 µmol.L^{-1}/µg.µL^{-1}), and asparagine (WT: 3.67 ± 0.32 vs. *Snat3*$^{-/-}$: 1.82 ± 0.24 µmol.L^{-1}/µg.µL^{-1}) were less abundant in the liver of *Snat3*$^{-/-}$ mice. These amino acids are important substrates in gluconeogenesis and glycogen synthesis [4] and serve as inter-organ carriers of nitrogen and carbon [9]. As SNAT3 has been demonstrated to be regulated by insulin and serum starvation in hepatocytes [34], we analysed blood glucose and insulin levels in *Snat3*$^{-/-}$, *Snat3*$^{+/-}$, and wildtype mice. In comparison to their wildtype littermates, mutant mice showed a significant decrease of blood

glucose and insulin levels suggesting that SNAT3 is involved in glucose homeostasis (Fig. 3A and B). Therefore, we next examined the expression of enzymes involved in hepatic gluconeogenesis. Phosphoenol pyruvate carboxykinase (PEPCK) was up-regulated significantly at both mRNA (Fig. 3C) and protein levels (Fig. 3F,G). In contrast, glutaminase 2 (GLS2) showed no changes at mRNA level (Fig. 3D) but the GLS2 protein was massively down-regulated in mutant mice (Fig. 3H,I). Surprisingly, glutamine synthetase 1 (GLU1) was strongly up-regulated at the mRNA level (Fig. 3E) but down-regulated at the protein level (Fig. 3J,K).

The mTOR pathway is reduced in Snat3 deficient mice.

Glutamine and other neutral amino acids are known to play a role in intracellular amino acid sensing. Since the mutant mice displayed altered plasma glucose and insulin levels and had reduced growth, we assumed that intracellular amino acid sensing via the mTOR pathway was affected [35-38]. Accordingly, leucine, phenylalanine, and tryptophane which can stimulate mTOR showed reduced levels in liver tissues of mutant mice (Fig. 4A-C). Additionally, the insulin-like growth factor 1 (IGF1) which is an activator of the mTOR pathway, was also down-regulated in *Snat3*-deficient mouse liver (Fig. 4D). Moreover, total and the phosphorylated forms of mTOR were massively down-regulated in mutant mice compared to wildtype littermates (Fig. 4E-H). Whereas the non-phosphorylated form of the ribosomal protein S6 kinase (S6K) showed no difference between genotypes, the phosphor-form of S6K was significantly less abundant in *Snat3*-deficient mice (Fig. 4I-L). The ratio of phospho-protein versus total protein was significantly lower in mutant mice for S6K whereas no difference was found for mTOR (Fig. 3M and N). This suggests that the decrease of phosphorylated mTOR parallels the decrease of total mTOR

expression whereas the decrease of phospho-S6K was due to a decrease in the phosphorylation state of this protein possibly because of a reduced mTOR activity.

Mutant Snat3 mice show an altered hepatic urea cycle.

The liver is responsible for detoxification of ammonia by converting it into urea through the urea cycle [6]. Because SNAT3 is highly expressed in liver and is likely to be involved in the urea cycle, we examined the hepatic urea cycle in the mutant mice. Serum urea levels were substantially increased in mutant mice in comparison to littermates (Fig. 5A) but no difference was observed in plasma ammonium levels between genotypes (Fig. 5B). Hepatic carbamoyl phosphatesynthetase I (*Cps1*) and ornithine-transcarbamylase (*Otc*) mRNA expression showed no significant differences in mutant mice compared to wildtype animals, whereas argininosuccinate lyase (*Asl*), and arginase I (*Arg1*) levels were significantly increased in mutant mice (Fig 5C-F).

The glutamate-glutamine cycle is defective in the brain of Snat3 deficient mice.

SNAT3 is highly expressed in brain astrocytes, and is believed to play a role in the glutamate-glutamine cycle involved in neurotransmission [5, 15, 22]. The lethargy and an altered, uncoordinated gait observed in mutant mice suggested impaired neurotransmission after *Snat3* deletion in brain. We thus measured the concentrations of different amino acids and neurotransmitters involved in the glutamate-glutamine cycle (Supplementary Table 4). Glutamine abundance was higher whereas glutamate and gamma-aminobutyric acid (GABA) levels were lower in brains of mutant animals (Fig. 6A-C). We also assessed the expression of the glutamine and glutamate transporters implicated in the glutamate-glutamine cycle.

The system A transporters *Snat1* and *Snat2* showed no difference at mRNA levels in mutant mice when compared to wildtype and heterozygous littermates (Fig. 6D and E). Yet, Snat1 is expressed exclusively in neurons [16, 39-40] and was significantly up-regulated in the brain of mutant mice at the protein level (Fig. 6J and K). The system N transporter *Snat5* was down-regulated at the mRNA level (Fig. 6F). No changes were observed at mRNA or protein levels in expression of any of the glutamate transporters Slc1a1 (Eaac1 or Eaat3) and Slc1a2 (Glt-1 or Eaat2) (Fig. 6G and H, L and M). The mRNA expression of glutamine synthetase (*Glu1*), which mediates the conversion of glutamate to glutamine in astrocytes, showed no difference between genotypes (Fig. 6I). Lastly, protein expression of the system L amino acid transporter 1 (LAT1) mediating the transport of neutral amino acids and expressed in brain vessels [41] and possibly also in neurons [42] was significantly increased in mutant mice when compared to wildtype (Fig. 6N and O).

Impaired ammoniagenic pathway in kidney.

We next investigated the involvement of SNAT3 in ammoniagenesis in the kidney. Glutamine and glutamate were both less abundant in kidneys of *Snat3*-deficient animals (Fig. 7A and B, Supplementary Table 5). Urine spot samples were collected as it was impossible to collect 24h urine samples from two-week old pups. Urinary NH_4^+ and urea excretion was significantly reduced in homozygous *Snat3* mutant mice in comparison to wildtype and heterozygous littermates (Fig. 7C and D). The enzymes involved in ammoniagenesis: phosphate-dependent glutaminase (*Pdg*) showed elevated levels but no change in phosphoenolpyruvate carboxykinase (*Pepck*) in *Snat3*$^{-/-}$ mice (Fig. 7E,F).

The RhCG transporter is primarily expressed in the connecting tubule and the collecting duct, and plays an important role in apical NH_4^+ extrusion into the final urine [43-44]. Mutant mice showed no changes in renal mRNA expression of Rhcg (Supplementary Fig. 1A). *Snat2* and *Snat5* are both highly expressed in the kidney and could potentially compensate for the loss of Snat3 function in mutant mice. However, no changes in mRNA expression were observed for *Snat2* (Supplementary Fig. 1B). In contrast, *Snat5* was significantly down-regulated in mutant mice compared to heterozygous and wildtype animals (Supplementary Fig. 1C). However, no specific antibodies were available to test protein abundance and renal localization. The system L Amino acid transporter 2 ( ), an antiporter for neutral amino acids expressed in the kidney [20] is likely involved in the efflux of glutamine from proximal tubular cells [28] and was found down-regulated at the protein level in mutant mice (Fig. 7G,H).

Since homozygous mutant mice are not viable enough to perform acid-loading tests to stimulate ammoniagenesis and because heterozygous mutant mice showed reduced Snat3 protein expression, we tested if 12 week old heterozygous mice could adapt renal ammoniagenesis. Wildtype and heterozygous mice were given NH_4Cl for two days to induce a metabolic acid load. Both groups of mice consumed similar amounts of the NH_4Cl drinking water and developed metabolic acidosis with similar falls in blood pH and blood bicarbonate (data not shown). Moreover, after 2 days of acid load, both wildtype and heterozygote mice showed a similar increase in total urinary NH_4^+ excretion (Fig. 8A) and a decrease in urinary pH (Fig. 8B). However, renal *Pdg* and *Pepck,* but not *Snat3*, showed significantly higher mRNA levels in heterozygote mice after acid-loading compared to wildtype mice (Fig. 8C-E. This

suggests that a higher induction of these enzymes may be required to reach the same level of ammoniagenesis as in wildtype animals.

DISCUSSION

This is the first report on the deletion of a member of the SLC38 family of glutamine transporters in an animal. Several members of the SLC38 family have been studied extensively in heterologous and other *in vitro* systems [18, 20, 23, 34] but their function *in vivo* is mainly unknown. Here we report a severe phenotype of mice lacking Snat3 due to an early stop codon introduced by random ENU-mutagenesis. Mice deficient of *Snat3* die early before weaning and display ataxia, multiple defects in amino acid homeostasis, glucose metabolism, glutamate-glutamine cycle, and renal ammoniagenesis. Together, these impairments might explain the early death of mutant mice after 20 days of life.

SNAT3 is an amino acid transporter with substrate specificity for glutamine, histidine, serine, and asparagine. Slc38a3 mutant mice had elevated plasma histidine levels whereas serine, glutamine, and asparagine levels remained unaltered. These data indicate that the alterations in the plasma amino acid profile most likely reflect secondary changes in cellular metabolism. Glutamine levels in plasma may be unaltered because the pool of glutamine is large and because SNAT3 most likely serves as uptake transporter into renal proximal tubule cells and hepatocytes using glutamine as substrate for the urea cycle and gluconeogenesis (see below). In brain, SNAT3 serves the local recycling of glutamine and disruption of this function is not expected to alter systemic glutamine levels.

Snat3 deficient mice suffered from altered energy metabolism. Homozygous mutant mice were hypoglycemic and the decrease in plasma glucose may originate from a reduced hepatic capacity for gluconeogenesis. The low insulin levels

measured would be the appropriate compensation for this primary fall in glucose levels. The lack of Snat3 significantly lowered hepatic glutamine levels with glutamine as a main substrate for gluconeogenesis. The decrease in plasma and hepatic alanine content, the decrease in plasma insulin, the up-regulation of the gluconeogenic enzyme Pepck as well as the down-regulation of Gls2 observed in *Snat3*-deficient animals points to an increased use of alanine as a glucogenic amino acid due to reduced availability of glutamine. Hence, changes in alanine concentrations are most likely to be a secondary effect of Snat3 deletion as alanine is not a substrate of SNAT3 [21, 45]. As the increased Snat5 expression observed disagrees with the decreased hepatic alanine content, Snat4 which is highly expressed in liver could explain this difference [46]. A previously unrecognized function of SNAT3 appears to be its role in histidine removal and metabolism by the liver. Liver is the main site of histidine metabolism, depending, at least in part, on uptake via SNAT3.

Snat3 deficient mice also exhibited changes in the mTOR/S6K signaling pathway that plays a major role in sensing of intracellular amino acids and is involved in regulation of protein synthesis, energy metabolism, cellular proliferation, and body growth [35-36, 38]. mTOR activity is particularly sensitive to the availability of essential amino acids such as tryptophan, phenylalanine, arginine and leucine as well as also to glutamine [47] but also to glucose, insulin and insulin like growth factor 1 (IGF1) levels [35]. Therefore, the decrease in glutamine, phenylalanine, tryptophan, glucose, insulin, and IGF1 availability observed in the Snat3-deficient mice could lead to the substantial reduction of the levels of the activated forms of both mTOR and S6K. Reduced activation of mTOR points to a collaboration between LAT1 and SNAT3 in providing amino acids for mTOR activation. Glutamine is taken by SNAT3

and can serve as an exchange substrate for leucine and tryptophan uptake by LAT1. Thus the role of SNAT3 in liver is similar to that of ASCT2 in cancer cells and SNAT2 in muscle cells [48-49]. Further, such a reduced mTOR signaling might be one reason why Snat3-deficient mice suffer from growth-retardation in the neonatal period [50].

SNAT3 properties and the cellular distribution within the liver suggest its involvement ammonia detoxification from the portal blood via the urea cycle [6, 21]. SNAT3 would deliver glutamine which is converted to glutamate which together with ammonium enters the urea cycle with urea finally excreted via kidneys. In the absence of Snat3, plasma ammonium levels remained unaltered whereas plasma urea levels were increased. We hypothesize that a reduced glutamine transport into periportal hepatocytes would result in a reduced NH_4^+ production from the catabolism of glutamine to glutamate with reduced levels of NH_4^+ available for ureagenesis. However, the increase in arginase (Arg1) and argininosuccinate lyase (Asl) observed in Snat3-deficient mice indicates that some compensatory mechanisms are in place to maintain urea production. Alternatively, low glucose levels may trigger increased protein catabolism to maintain energy production and the elevated urea levels and higher expression of enzymes may reflect enhanced formation of NH_4^+ from protein break-down. A third possibility would be decreased renal clearance of urea [51], however, creatinine levels were in the normal range suggesting that renal function was not completely disturbed. Thus, the higher urea levels may be the result of disturbances at various levels and the early death of mutant animals complicates a detailed analysis.

In brain, the deletion of Snat3 caused changes in the expression of several amino acid transporters as well of amino acid and neurotransmitter levels consistent

with a major role of the protein in the glutamate-glutamine cycle. Disrupted neurotransmitter synthesis could also explain the neurological disturbances seen in the Snat3-deficient mice. Glutamate released into the synapse is taken up by surrounding astrocytes via the Slc1a2 (Eaat2/Glt1) and Slc1a3 (Eaat1/Glast) glutamate transporters. Some glutamate is also taken up by Slc1a1 (Eaat3/Eaac1) transporters localized in neurons. After the conversion of glutamate to glutamine by glutamine synthetase, glutamine is released, possibly via Snat3 and/or Snat5 and taken up by neurons which may involve the Snat1 and Snat2 glutamine transporters for reconversion to glutamate by glutaminases [5, 15-17, 22, 42, 52-53]. The absence of Snat3 in the brain of mutant animals could therefore impair the release of glutamine from astrocytes and thereby affecting neuronal glutamate and GABA synthesis. The accumulation of glutamine correlated with the decrease of GABA and glutamate in the brain of mutant mice. The observed up-regulation of Snat1 and Lat1 in mutant mice, which are thought to be involved in the uptake of glutamine into neurons and the release of glutamine from astrocytes, respectively, could be taken as an indicator of compensatory mechanisms. Concentrations of tyrosine and tryptophane, which are precursors of important neurotransmitters involved in cognitive functions, such as serotonin and dopamine, respectively, displayed reduced levels in mutant brain. Furthermore, the decrease of brain alanine concentrations might be explained by an increased Snat1-mediated alanine uptake as an additional source for glutamate synthesis [54]. Snat3 is also expressed in the endothelium of the blood brain barrier [19]. The elevated levels of glutamine in brain tissues may suggest that the main function of Snat3 at the blood-brain barrier is not the import of glutamine into the cerebro-spinal but the efflux of glutamine in coupling to other amino acid exchangers. Altogether, our results implicate Snat3 as critical if not as the

major facilitator of glutamine efflux from astrocytes in supply of glutamine for neurotransmitter synthesis. Cell-specific deletions of Snat3 and other members of the SLC38 family in brain are required to define their specific functions in neurotransmission.

In the kidney, glutamine is the primary metabolic source for the release of NH_3, which when excreted as NH_4^+ helps to save CO_2 for de-novo synthesis of bicarbonate to restore systemic acid-base balance. Uptake of glutamine for ammoniagenesis has been attributed to Snat3 because Snat3 shows induction in parallel to increased ammoniagenesis [18, 20, 23]. Snat3-deficient mice showed a decrease in urinary ammonium excretion consistent with impaired ammoniagenesis. The up-regulation of the phosphate-dependent glutaminase (Pdg) as well as the down-regulation of Lat2 as a basolateral efflux pathway for glutamine, are likely a result of compensatory mechanisms to correct the decrease in glutamine availability. Similarly, the observed up-regulation in Pepck protein expression in kidney might indicate a compensation for a decrease of α-ketoglutarate availability. On the other hand, fasting increases *Pepck*-mRNA - apparently not reverted by glucose or insulin but by bicarbonate [55]. This suggests that increased Pepck in kidney are a measure of acidosis by impaired ammoniagenesis rather than of increased gluconeogenesis [55]. The early lethality in homozygous mutants made it impossible to conduct further metabolic experiments on renal functions. Since heterozygotic mice had reduced expression of SNAT3 we tested whether a partial defect in Snat3 could be functionally relevant during an oral acid load. Heterozygous mice showed similar changes in urinary pH and NH_4^+ excretion as wildtype animals. However, heterozygous mice obviously required a higher induction of *Pdg* and *Pepck* mRNA

expression to achieve similar NH_4^+ excretion rates suggesting that the partial loss of Snat3 impacts on ammoniagenesis.

In conclusion, our results demonstrate that SNAT3 is a transporter for glutamine that is crucial for amino acid homeostasis in brain, liver and kidney. Moreover, signaling processes that mediate growth such as the mTOR/S6K pathway revealed changes that may also explain the retarded growth of animals lacking Slc38a3. Early lethality in mice prevented detailed analysis of organ-specific alterations and thus future studies on the physiological importance of SNAT3 and of glutamine need tissue-and cell-type specific deficiencies.

Competing interests

The authors declare that they have no conflicts of interest to declare.

Acknowledgements

We thank François Verrey (Institute of Physiology, University of Zurich, Switzerland) for providing us with anti-SNAT1 and anti-SNAT3 antibodies, and Norman Curthoys, (Department of Biochemistry and Molecular Biology, Colorado State University, Fort Collins, CO, USA) for providing us with the anti-PDG antibody. This study was supported by grants from the 6th EU frame work project EUGINDAT and the Swiss National Science Foundation (31003A_155959/1) to C.A. Wagner.

FIGURE LEGENDS

FIGURE 1

Snat3 point mutation leads to loss of Snat3 protein expression **(*A*)** Relative *Snat3* mRNA expression in different organs of wildtype animals, n = 3. **(*B*)** Schematic model of the Snat3 transporter indicating the localization of the "C" to "T" mutation, "Slc38a3-Q263X", causing a premature stop codon deleting the second half of the protein. The numbers below indicate the putative transmembrane domains. **(*C*)** At day 14 after birth, mutant animals were significantly smaller than wildtype (WT) animals **(D,E,F)** Relative mRNA expression of *Snat3* was determined in brain, liver and kidney of wildtype, hetereozygous (*Snat3*$^{+/-}$) and mutant (*Snat3*$^{-/-}$) mice, n = 10-12/genotype. **(*G,H,I*)** Protein expression of Snat3 was assessed in total membrane fractions from brain, liver and kidney. Snat3 protein was not detectable in the brain, liver and kidney of homozygous mutant animals (*Snat3*$^{-/-}$) and reduced in heterozygous (*Snat3*$^{+/-}$) mice. All blots were tested for equal loading with β-actin after stripping of membranes. **(*I*)** Presence of Snat3 (red) and Ace2 (green) staining in kidneys from wildtype animals and absence of Snat3 staining from homozygous mutant kidney. **P* ≤ 0.05, ***P ≤ 0.001.

FIGURE 2

Plasma amino acid concentrations. Plasma amino acid concentrations were determined in 14 days old mice, all values are given in µmol/L, wildtype (WT) and homozygous mutant (*Snat3*$^{-/-}$) mice (n = 6). **P* ≤ 0.05, **P ≤ 0.01, ***P ≤ 0.001.

FIGURE 3

Absence of Snat3 causes hypoglycemia and affects hepatic amino acid and glucose metabolism **(*A*)** Plasma glucose in *ad libitum* feeding mice was lower in homozygous mutant (*Snat3*$^{-/-}$) mice, n = 8-27/genotype **(*B*)** Plasma insulin concentration in *ad libitum* feeding mice was reduced in homozygous mutant (*Snat3*$^{-/-}$

) animals, n = 9/genotype. **(*C,D,E*)** mRNA abundance of phosphoenolpyruvate carboxykinase (*Pepck*) was upregulated whereas glutamine synthetase (*Glu1*) and (*Gls2)* were downregulated at mRNA level in Snat3 deficient animals. **(F-K)** Expression of the phosphoenolpyruvate carboxykinase (Pepck) was increased whereas the abundance of glutaminase 2 (Gls2) and glutamine synthetase (Glu1) was downregulated. All blots were reprobed for β-actin to control for loading and β-actin used for calculation of relative abundance. Normalized data are presented as bar graphs showing mean ± SEM. n = 11-12/genotype for qPCR, n = 5-6/genotype for immunoblots, **P* ≤ 0.05, ***P* ≤ 0.01, ***P ≤ 0.001.

FIGURE 4

Snat3 mutant mice showed a disrupted hepatic mTOR/S6K pathway. **(*A, B, C*)** Quantification of hepatic amino acid concentrations for leucine (Leu), phenylalanine (Phe) and tryptophane (Trp), normalized against total protein ($\mu mol.L^{-1}/\mu g.\mu L^{-1}$), n = 6/genotype. **(*D*)** Insulin-like growth factor 1 (*Igf1*) was significantly downregulated at mRNA level in homozygous mutant (*Snat3*$^{-/-}$*)*, n = 11-12/genoytpe. ***(E-F)*** Bar graphs showing ratios of phosphorylated proteins to total proteins. ***(G-N)*** Immunoblotting for hepatic total non-phosphorylated and phosphorylated mammalian target of rapamycin (mTOR) and S6 Kinase (S6K). All blots were reprobed for β-tubuline or β-actin to control for loading. Bar graphs show means ± SEM of the ratio of the protein of interest over loading control. Both total non-phosphorylated and phosphorylated mTOR were significantly downregulated in homozygous mutant *Snat3* mice. Total S6K showed no difference in all mice, but phosphorylated S6K was massively reduced in Snat3 deficient mice. **P* ≤ 0.05, ***P* ≤ 0.01

FIGURE 5

Snat3 deficiency affects urea cycle and metabolism. **(*A*)** Urea was significantly increased in the plasma of Snat3 deficient mice, n = 5-13/genotype. **(*B*)** Plasma ammonium levels were unchanged in all genotypes, n = 9-10/genotype. **(*C-F*)** mRNA expression of enzymes involved in the urea cycle. Carbamoyl phosphate synthetase I (Cps1) and ornithine transcarbamoylase (Otc) and were not altered, whereas

argininosuccinate lyase (*Asl*) and arginase 1 (*Arg1)* were upregulated in the liver from Snat3 deficient animals n = 11-12/genotype. **P* ≤ 0.05.

FIGURE 6

Loss of Snat3 in the brain reduces neurotransmitter abundance and stimulates alternative transporter expression. **(*A, B, C*)** Quantification of amino acid concentrations in the brain. Brain of homozygous mutant *Snat3* animals showed increased glutamine (Gln) levels but lower abundance of glutamate (Glu) and gamma-aminobutyric acid (GABA). Amino acid levels were normalized to total protein content ($\mu mol.L^{-1}/\mu g.\mu L^{-1}$), n = 6. **(*D-I*)** Brain mRNA expression of the sodium-coupled neutral amino acid transporter 1 (*Snat1), 2 (Snat2)*, and 5 (*Snat5),* the excitatory amino-acid transporter 3 *(Slc1a1),* the excitatory amino-acid transporter 2 (*Slc1a2*), and glutamine synthetase (*Glu1*) were measured by RT-qPCR in all mice and only Snat5 mRNA was significantly reduced in Snat3 deficient mice, n = 10-12/genotype. **(*J-O*)** Immunoblotting for the sodium-coupled neutral amino acid transporter 1 (Snat1), the excitatory amino-acid transporter 2 (Slc1a2), and the large neutral amino acid transporter 1 (Lat1). All membranes were reprobed for β-actin to control for loading. Normalized protein expression was calculated and is shown in bar graphs. The glutamate transporter Slc1a2 showed no difference but Snat1 and Lat1 were upregulated in brains from Snat3 deficient mice. n=5/genotype, **P* ≤ 0.05, ***P* ≤ 0.01.

FIGURE 7

Deletion of Snat3 affects renal ammoniagenesis and reduces urinary ammonium excretion. **(*A, B*)** Quantification of renal amino acid concentrations per total protein ($\mu mol.L^{-1}/\mu g.\mu L^{-1}$). Glutamine (Gln) and Glutamate (Glu) levels were both reduced in the kidneys of Snat3 deficient animals, n = 6/genotype. **(*C, D*)** Homozygous *Snat3* mutant mice showed reduced urinary NH_4^+ and urea excretion normalized to creatinine in the urine, n = 6-14/genotype. **(*E,F*)** Immunoblotting of phosphate dependent glutaminase (Pdg) and renal phosphoenolpyruvate carboxykinase (Pepck), n = 4/genotype. Pepck showed no difference but Pdg was upregulated in kidneys form Snat3 deficient mice. **(*J,K*)** Reduced expression of the

large neutral amino acid transporter 2 (Lat2) in the kidneys of Snat3 deficient mice. The membrane was reprobed for β-actin to control for loading. Bar graph shows normalized protein expression.

FIGURE 8

Altered expression of key players of the ammoniagenic pathway in acid loaded Snat3 heterozygous mice. (A-E) Wildtype and *Snat3* heterozygous mice were challenged with an oral acid load (NH_4Cl) for 2 days. Both wildtype and heterozygous mice increased NH_4^+ excretion per 24-hour urine, n = 4-6. Acid-challenged *Snat3* heterozygous mice showed a more pronounced increase in *Pepck, Pdg* but not *Snat3* mRNA expression, n = 4-6/genotype. WT (displayed in white), WT after 2 days NH_4Cl load (displayed in light grey), *Snat3*$^{-/-}$ (displayed in black), after 2 days NH_4Cl load (displayed in dark grey). **P* ≤ 0.05, ***P* ≤ 0.01, ***P ≤ 0.001.

REFERENCES

1. Wu G (2009) Amino acids: metabolism, functions, and nutrition. Amino Acids 37:1-17 DOI 10.1007/s00726-009-0269-0

2. Curi R, Newsholme P, Procopio J, Lagranha C, Gorjao R, Pithon-Curi TC (2007) Glutamine, gene expression, and cell function. Front Biosci 12:344-57 DOI 2068 [pii]

3. Curi R, Lagranha CJ, Doi SQ, Sellitti DF, Procopio J, Pithon-Curi TC, Corless M, Newsholme P (2005) Molecular mechanisms of glutamine action. J Cell Physiol 204:392-401 DOI 10.1002/jcp.20339

4. Stumvoll M, Perriello G, Meyer C, Gerich J (1999) Role of glutamine in human carbohydrate metabolism in kidney and other tissues. Kidney Int 55:778-92 DOI 10.1046/j.1523-1755.1999.055003778.x

5. McKenna MC (2007) The glutamate-glutamine cycle is not stoichiometric: fates of glutamate in brain. J Neurosci Res 85:3347-58 DOI 10.1002/jnr.21444

6. Haussinger D, Schliess F (2007) Glutamine metabolism and signaling in the liver. Front Biosci 12:371-91 DOI 2070 [pii]

7. Welbourne TC, Matthews JC (1999) Glutamate transport and renal function. Am J Physiol 277:F501-5 DOI

8. Li P, Yin YL, Li D, Kim SW, Wu G (2007) Amino acids and immune function. Br J Nutr 98:237-52 DOI S000711450769936X [pii]
10.1017/S000711450769936X

9. Nurjhan N, Bucci A, Perriello G, Stumvoll M, Dailey G, Bier DM, Toft I, Jenssen TG, Gerich JE (1995) Glutamine: a major gluconeogenic precursor and vehicle for interorgan carbon transport in man. J Clin Invest 95:272-7 DOI 10.1172/JCI117651

10. Welbourne TC, Childress D, Givens G (1986) Renal regulation of interorgan glutamine flow in metabolic acidosis. Am J Physiol 251:R859-66 DOI

11. Kanai Y, Clemencon B, Simonin A, Leuenberger M, Lochner M, Weisstanner M, Hediger MA (2013) The SLC1 high-affinity glutamate and neutral amino acid transporter family. Mol Aspects Med 34:108-20 DOI S0098-2997(13)00002-2 [pii]
10.1016/j.mam.2013.01.001

12. Broer S (2008) Amino acid transport across mammalian intestinal and renal epithelia. Physiol Rev 88:249-86 DOI 88/1/249 [pii]
10.1152/physrev.00018.2006

13. Broer S (2014) The SLC38 family of sodium-amino acid co-transporters. Pflugers Arch 466:155-72 DOI 10.1007/s00424-013-1393-y

14. Albers A, Broer A, Wagner CA, Setiawan I, Lang PA, Kranz EU, Lang F, Broer S (2001) Na+ transport by the neural glutamine transporter ATA1. Pflugers Arch 443:92-101 DOI 10.1007/s004240100663

15. Chaudhry FA, Krizaj D, Larsson P, Reimer RJ, Wreden C, Storm-Mathisen J, Copenhagen D, Kavanaugh M, Edwards RH (2001) Coupled and uncoupled proton movement by amino acid transport system N. EMBO J 20:7041-51 DOI 10.1093/emboj/20.24.7041

16. Chaudhry FA, Schmitz D, Reimer RJ, Larsson P, Gray AT, Nicoll R, Kavanaugh M, Edwards RH (2002) Glutamine uptake by neurons: interaction of protons with system a transporters. J Neurosci 22:62-72 DOI 22/1/62 [pii]

17. Chaudhry FA, Reimer RJ, Krizaj D, Barber D, Storm-Mathisen J, Copenhagen DR, Edwards RH (1999) Molecular analysis of system N suggests novel physiological roles in nitrogen metabolism and synaptic transmission. Cell 99:769-80 DOI

18. Solbu TT, Boulland JL, Zahid W, Lyamouri Bredahl MK, Amiry-Moghaddam M, Storm-Mathisen J, Roberg BA, Chaudhry FA (2005) Induction and targeting of the glutamine transporter SN1 to the basolateral membranes of cortical kidney tubule cells during chronic metabolic acidosis suggest a role in pH regulation. J Am Soc Nephrol 16:869-77 DOI

19. Ruderisch N, Virgintino D, Makrides V, Verrey F (2011) Differential axial localization along the mouse brain vascular tree of luminal sodium-dependent glutamine transporters Snat1 and Snat3. J Cereb Blood Flow Metab 31:1637-47 DOI jcbfm201121 [pii]
10.1038/jcbfm.2011.21

20. Moret C, Dave MH, Schulz N, Jiang JX, Verrey F, Wagner CA (2007) Regulation of renal amino acid transporters during metabolic acidosis. Am J Physiol Renal Physiol 292:F555-66 DOI 00113.2006 [pii]
10.1152/ajprenal.00113.2006

21. Gu S, Roderick HL, Camacho P, Jiang JX (2000) Identification and characterization of an amino acid transporter expressed differentially in liver. Proc Natl Acad Sci U S A 97:3230-5 DOI 10.1073/pnas.050318197
050318197 [pii]

22. Boulland JL, Osen KK, Levy LM, Danbolt NC, Edwards RH, Storm-Mathisen J, Chaudhry FA (2002) Cell-specific expression of the glutamine transporter SN1 suggests differences in dependence on the glutamine cycle. Eur J Neurosci 15:1615-31 DOI 1995 [pii]

23. Busque SM, Wagner CA (2009) Potassium restriction, high protein intake, and metabolic acidosis increase expression of the glutamine transporter SNAT3 (Slc38a3) in mouse kidney. Am J Physiol Renal Physiol 297:F440-50 DOI 90318.2008 [pii]
10.1152/ajprenal.90318.2008

24. Nowik M, Lecca MR, Velic A, Rehrauer H, Brandli AW, Wagner CA (2008) Genome-wide gene expression profiling reveals renal genes regulated during metabolic acidosis. Physiol Genomics 32:322-34 DOI

25. Welbourne T, Weber M, Bank N (1972) The effect of glutamine administration on urinary ammonium excretion in normal subjects and patients with renal disease. J Clin Invest 51:1852-60 DOI 10.1172/JCI106987

26. Haser WG, Shapiro RA, Curthoys NP (1985) Comparison of the phosphate-dependent glutaminase obtained from rat brain and kidney. Biochem J 229:399-408 DOI

27. Campbell WA, Sah, D E, Medina, M M, Albina, J E, Coleman, W B, Thompson, N L (2000) TA1/LAT-1/CD98 light chain and system L activity, but not 4F2/CD98 heavy chain, respond to arginine availability in rat hepatic cells. Loss of response in tumor cells. J Biol Chem 275:5347-54 DOI

28. Rossier G, Meier, C, Bauch, C, Summa, V, Sordat, B, Verrey, F, Kühn, L C (1999) LAT2, a new basolateral 4F2hc/CD98-associated amino acid transporter of kidney and intestine. J Biol Chem 274:34948-54 DOI

29. Sailer M, Dahlhoff C, Giesbertz P, Eidens MK, de Wit N, Rubio-Aliaga I, Boekschoten MV, Muller M, Daniel H (2013) Increased plasma citrulline in mice marks diet-induced obesity and may predict the development of the metabolic syndrome. PLoS One 8:e63950 DOI 10.1371/journal.pone.0063950
PONE-D-12-31988 [pii]

30. Nowik M, Kampik NB, Mihailova M, Eladari D, Wagner CA (2010) Induction of metabolic acidosis with ammonium chloride (NH4Cl) in mice and rats--species differences and technical considerations. Cell Physiol Biochem 26:1059-72 DOI 000323984 [pii]
10.1159/000323984

31. Slot C (1965) Plasma creatinine determination. A new and specific Jaffe reaction method. Scand J Clin Lab Invest 17:381-7 DOI

32. Berthelot M (1859) Violet d'aniline. . Rep Chim App 1:284 DOI

33. Hrabe de Angelis MH, Flaswinkel H, Fuchs H, Rathkolb B, Soewarto D, Marschall S, Heffner S, Pargent W, Wuensch K, Jung M, Reis A, Richter T, Alessandrini F, Jakob T, Fuchs E, Kolb H, Kremmer E, Schaeble K, Rollinski B, Roscher A, Peters C, Meitinger T, Strom T, Steckler T, Holsboer F, Klopstock T, Gekeler F, Schindewolf C, Jung T, Avraham K, Behrendt H, Ring J, Zimmer A, Schughart K, Pfeffer K, Wolf E, Balling R (2000) Genome-wide, large-scale production of mutant mice by ENU mutagenesis. Nat Genet 25:444-7 DOI 10.1038/78146

34. Gu S, Villegas CJ, Jiang JX (2005) Differential regulation of amino acid transporter SNAT3 by insulin in hepatocytes. J Biol Chem 280:26055-62 DOI

35. Laplante M, Sabatini DM (2012) mTOR signaling in growth control and disease. Cell 149:274-93 DOI S0092-8674(12)00351-0 [pii]
10.1016/j.cell.2012.03.017

36. Laplante M, Sabatini DM (2009) mTOR signaling at a glance. J Cell Sci 122:3589-94 DOI 122/20/3589 [pii]
10.1242/jcs.051011

37. Cardenas ME, Cutler NS, Lorenz MC, Di Como CJ, Heitman J (1999) The TOR signaling cascade regulates gene expression in response to nutrients. Genes Dev 13:3271-9 DOI

38. Kim DH, Sarbassov DD, Ali SM, King JE, Latek RR, Erdjument-Bromage H, Tempst P, Sabatini DM (2002) mTOR interacts with raptor to form a nutrient-sensitive complex that signals to the cell growth machinery. Cell 110:163-75 DOI S0092867402008085 [pii]

39. Varoqui H, Zhu H, Yao D, Ming H, Erickson JD (2000) Cloning and functional identification of a neuronal glutamine transporter. J Biol Chem 275:4049-54 DOI

40. Mackenzie B, Erickson JD (2004) Sodium-coupled neutral amino acid (System N/A) transporters of the SLC38 gene family. Pflugers Arch 447:784-95 DOI

41. Duelli R, Enerson BE, Gerhart DZ, Drewes LR (2000) Expression of large amino acid transporter LAT1 in rat brain endothelium. J Cereb Blood Flow Metab 20:1557-62 DOI 10.1097/00004647-200011000-00005

42. Heckel T, Broer A, Wiesinger H, Lang F, Broer S (2003) Asymmetry of glutamine transporters in cultured neural cells. Neurochem Int 43:289-98 DOI S0197018603000147 [pii]

43. Bourgeois S, Bounoure L, Christensen EI, Ramakrishnan SK, Houillier P, Devuyst O, Wagner CA (2013) Haploinsufficiency of the ammonia transporter Rhcg predisposes to chronic acidosis: Rhcg is critical for apical and basolateral ammonia transport in the mouse collecting duct. J Biol Chem 288:5518-29 DOI M112.441782 [pii]
10.1074/jbc.M112.441782

44. Biver S, Belge H, Bourgeois S, Van Vooren P, Nowik M, Scohy S, Houillier P, Szpirer J, Szpirer C, Wagner CA, Devuyst O, Marini AM (2008) A role for Rhesus factor Rhcg in renal ammonium excretion and male fertility. Nature 456:339-43 DOI

45. Bröer S (2014 (in press)) The SLC38 family of sodium-amino acid cotransporters. Pflügers Arch

46. Varoqui H, Erickson JD (2002) Selective up-regulation of system a transporter mRNA in diabetic liver. Biochem Biophys Res Commun 290:903-8 DOI 10.1006/bbrc.2001.6281

47. Nicklin P BP, Zhang B, Triantafellow E, Wang H, Nyfeler B, Yang H, Hild M, Kung C, Wilson C, Myer VE, MacKeigan JP, Porter JA, Wang YK, Cantley LC, Finan PM, Murphy LO. (2009) Bidirectional transport of amino acids regulates mTOR and autophagy. Cell.;136(3):521-34. DOI

48. Fuchs BC, Finger RE, Onan MC, Bode BP (2007) ASCT2 silencing regulates mammalian target-of-rapamycin growth and survival signaling in human hepatoma cells. Am J Physiol Cell Physiol 293:C55-63 DOI 00330.2006 [pii]
10.1152/ajpcell.00330.2006

49. Evans K, Nasim Z, Brown J, Butler H, Kauser S, Varoqui H, Erickson JD, Herbert TP, Bevington A (2007) Acidosis-sensing glutamine pump SNAT2 determines amino acid levels and mammalian target of rapamycin signalling to protein synthesis in L6 muscle cells. J Am Soc Nephrol 18:1426-36 DOI ASN.2006091014 [pii] 10.1681/ASN.2006091014

50. Zoncu R, Efeyan A, Sabatini DM (2011) mTOR: from growth signal integration to cancer, diabetes and ageing. Nat Rev Mol Cell Biol 12:21-35 DOI nrm3025 [pii] 10.1038/nrm3025

51. Aigner B, Rathkolb B, Herbach N, Kemter E, Schessl C, Klaften M, Klempt M, de Angelis MH, Wanke R, Wolf E (2007) Screening for increased plasma urea levels in a large-scale ENU mouse mutagenesis project reveals kidney disease models. Am J Physiol Renal Physiol 292:F1560-7 DOI 00213.2006 [pii] 10.1152/ajprenal.00213.2006

52. Magistretti PJ, Pellerin L, Rothman DL, Shulman RG (1999) Energy on demand. Science 283:496-7 DOI

53. Conti F, Melone M (2006) The glutamine commute: lost in the tube? Neurochem Int 48:459-64 DOI S0197-0186(06)00038-6 [pii] 10.1016/j.neuint.2005.11.016

54. Erecinska M, Nelson D, Nissim I, Daikhin Y, Yudkoff M (1994) Cerebral alanine transport and alanine aminotransferase reaction: alanine as a source of neuronal glutamate. J Neurochem 62:1953-64 DOI

55. Iynedjian PB, Ballard FJ, Hanson RW (1975) The regulation of phosphoenolpyruvate carboxykinase (GTP) synthesis in rat kidney cortex. The role of acid-base balance and glucocorticoids. J Biol Chem 250:5596-603 DOI

Fig1

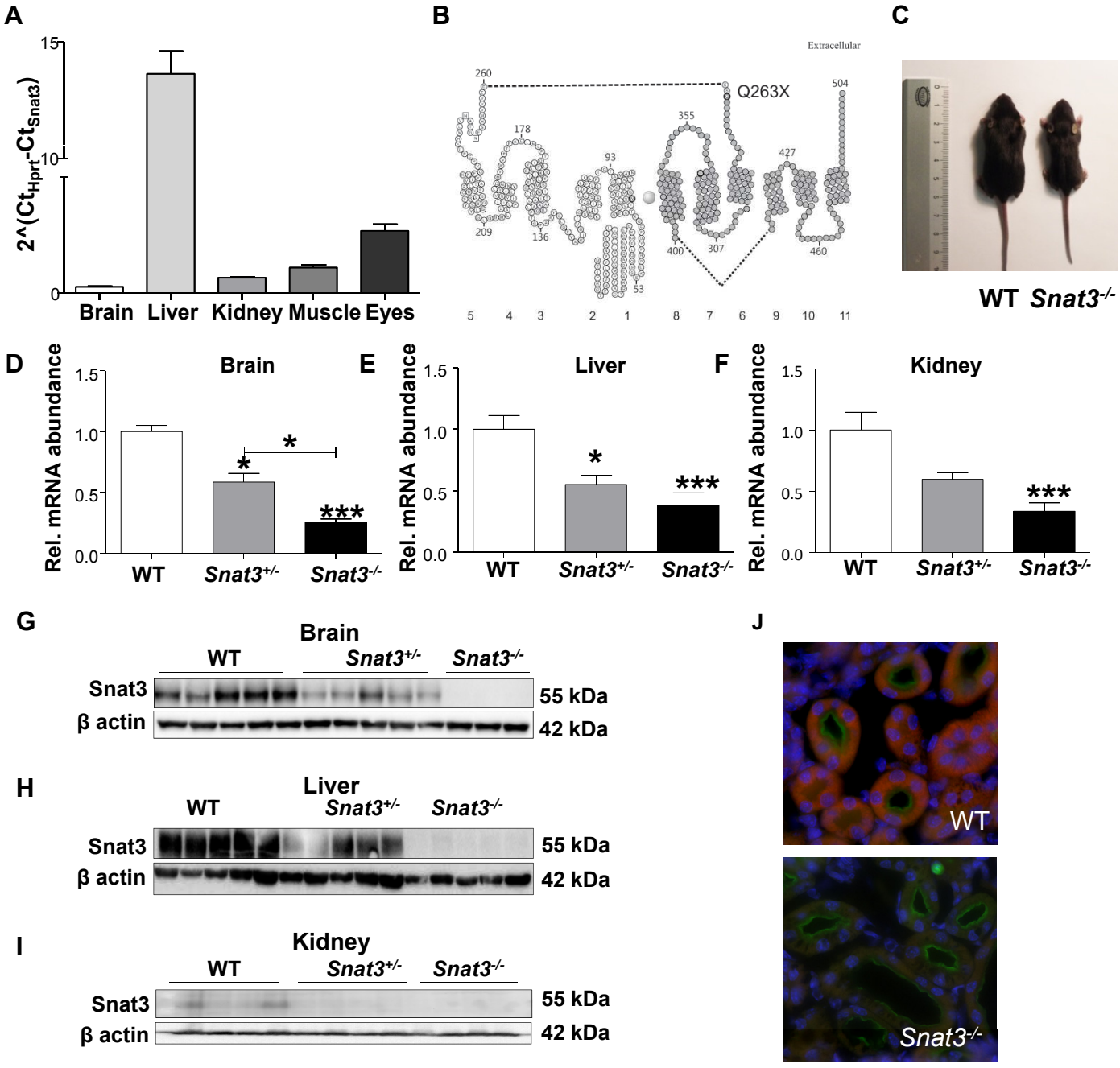
A
2^(Ct_Hprt-Ct_Snat3)
15
10
0
Brain
Liver
Kidney
Muscle
Eyes
B
Extracellular
Q263X
260
178
93
355
427
504
209
136
53
400
307
460
5
4
3
2
1
8
7
6
9
10
11
C
WT Snat3-/-
D
Brain
Rel. mRNA abundance
1.5
1.0
0.5
0.0
*
*
***
WT
Snat3+/-
Snat3-/-
E
Liver
Rel. mRNA abundance
1.5
1.0
0.5
0.0
*
***
WT
Snat3+/-
Snat3-/-
F
Kidney
Rel. mRNA abundance
1.5
1.0
0.5
0.0
***
WT
Snat3+/-
Snat3-/-
G
Brain
WT
Snat3+/-
Snat3-/-
Snat3
β actin
55 kDa
42 kDa
H
Liver
WT
Snat3+/-
Snat3-/-
Snat3
β actin
55 kDa
42 kDa
I
Kidney
WT
Snat3+/-
Snat3-/-
Snat3
β actin
55 kDa
42 kDa
J
WT
Snat3-/-

Fig2

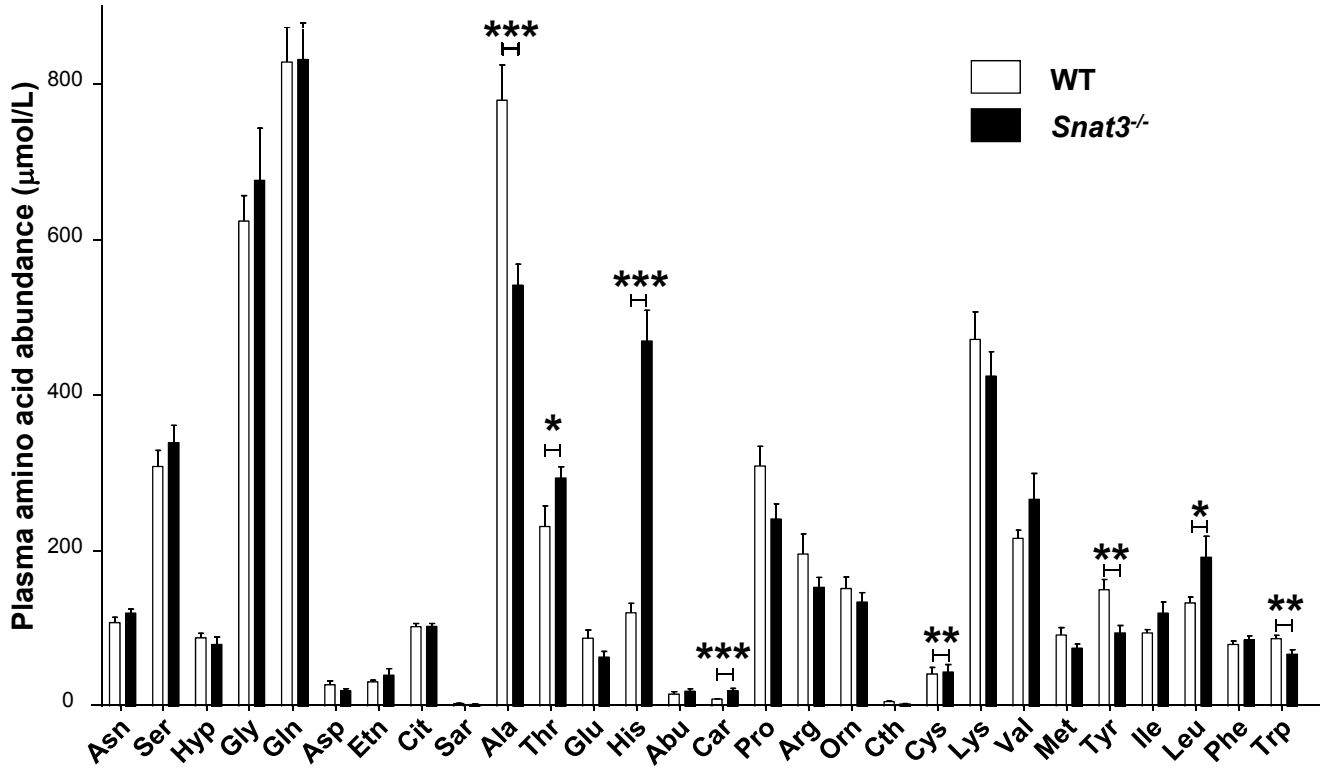
Plasma amino acid abundance (μmol/L)
0
200
400
600
800
WT
Snat3-/-
***
*
***
***
**
**
*
**
Asn
Ser
Hyp
Gly
Gln
Asp
Etn
Cit
Sar
Ala
Thr
Glu
His
Abu
Car
Pro
Arg
Orn
Cth
Cys
Lys
Val
Met
Tyr
Ile
Leu
Phe
Trp

Fig3

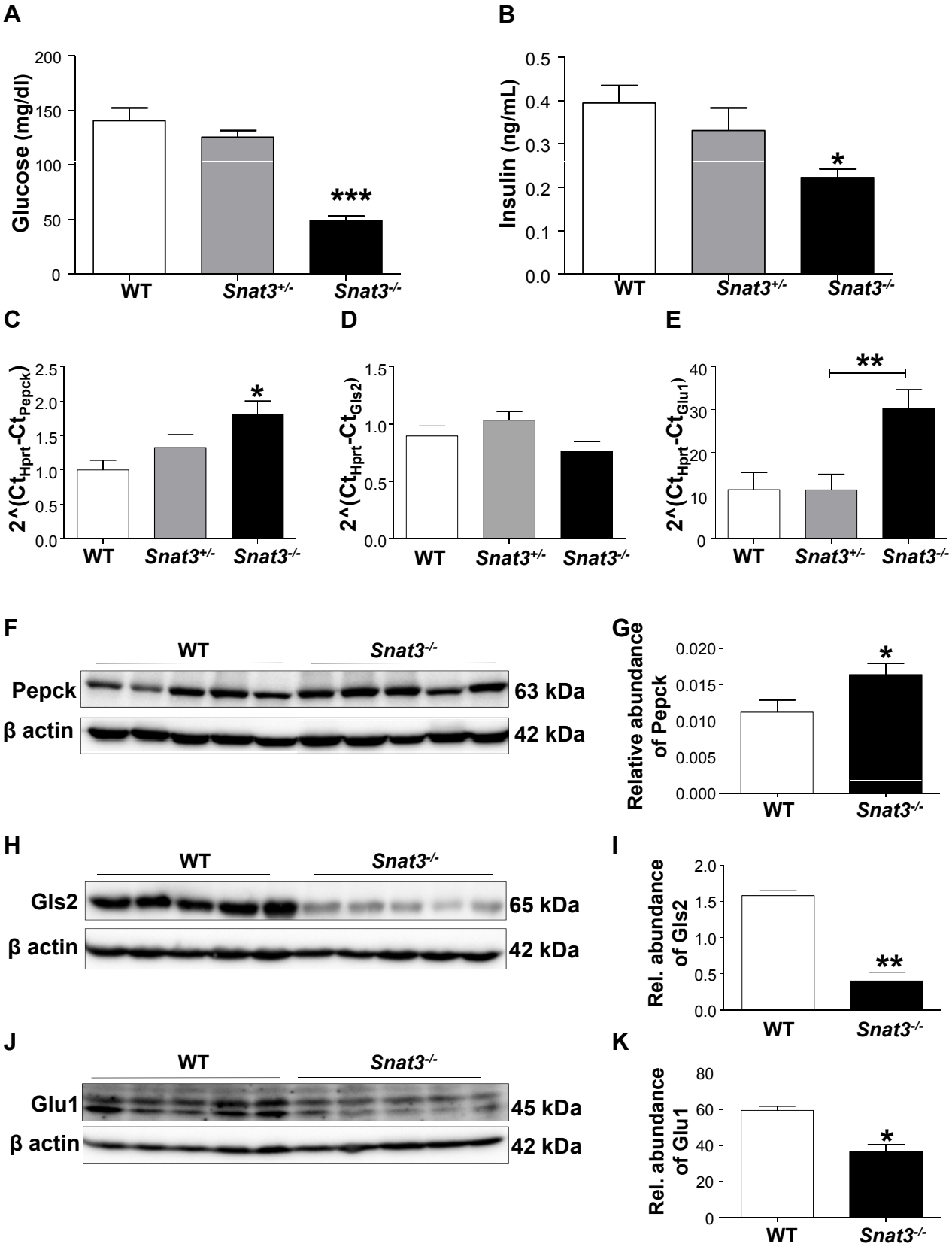
A
Glucose (mg/dl)
200
150
100
50
0
***
WT
Snat3+/-
Snat3-/-
B
Insulin (ng/mL)
0.5
0.4
0.3
0.2
0.1
0.0
*
WT
Snat3+/-
Snat3-/-
C
2^(Ct Hprt-Ct Pepck)
2.5
2.0
1.5
1.0
0.5
0.0
*
WT
Snat3+/-
Snat3-/-
D
2^(Ct Hprt-Ct Gls2)
1.5
1.0
0.5
0.0
WT
Snat3+/-
Snat3-/-
E
2^(Ct Hprt-Ct Glu1)
40
30
20
10
0
**
WT
Snat3+/-
Snat3-/-
F
WT
Snat3-/-
Pepck
63 kDa
β actin
42 kDa
G
Relative abundance of Pepck
0.020
0.015
0.010
0.005
0.000
*
WT
Snat3-/-
H
WT
Snat3-/-
Gls2
65 kDa
β actin
42 kDa
I
Rel. abundance of Gls2
2.0
1.5
1.0
0.5
0.0
**
WT
Snat3-/-
J
WT
Snat3-/-
Glu1
45 kDa
β actin
42 kDa
K
Rel. abundance of Glu1
80
60
40
20
0
*
WT
Snat3-/-

Fig4

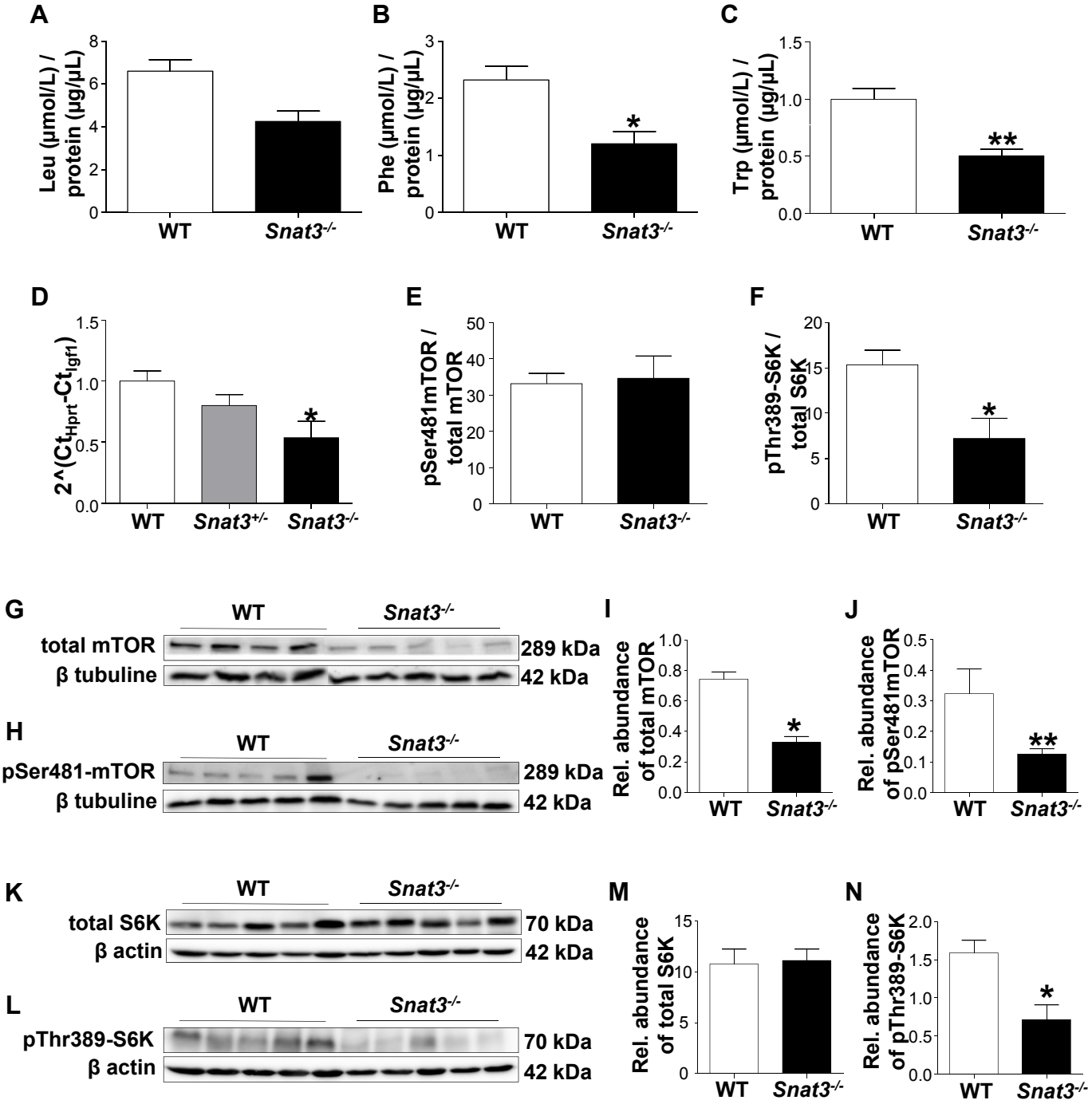
A
Leu (μmol/L) / protein (μg/μL)
WT
Snat3-/-
B
Phe (μmol/L) / protein (μg/μL)
C
Trp (μmol/L) / protein (μg/μL)
D
2^(Ct Hprt-Ct Igf1)
Snat3+/-
E
pSer481mTOR / total mTOR
F
pThr389-S6K / total S6K
G
total mTOR
β tubuline
289 kDa
42 kDa
H
pSer481-mTOR
I
Rel. abundance of total mTOR
J
Rel. abundance of pSer481mTOR
K
total S6K
β actin
70 kDa
L
pThr389-S6K
M
Rel. abundance of total S6K
N
Rel. abundance of pThr389-S6K

Fig5

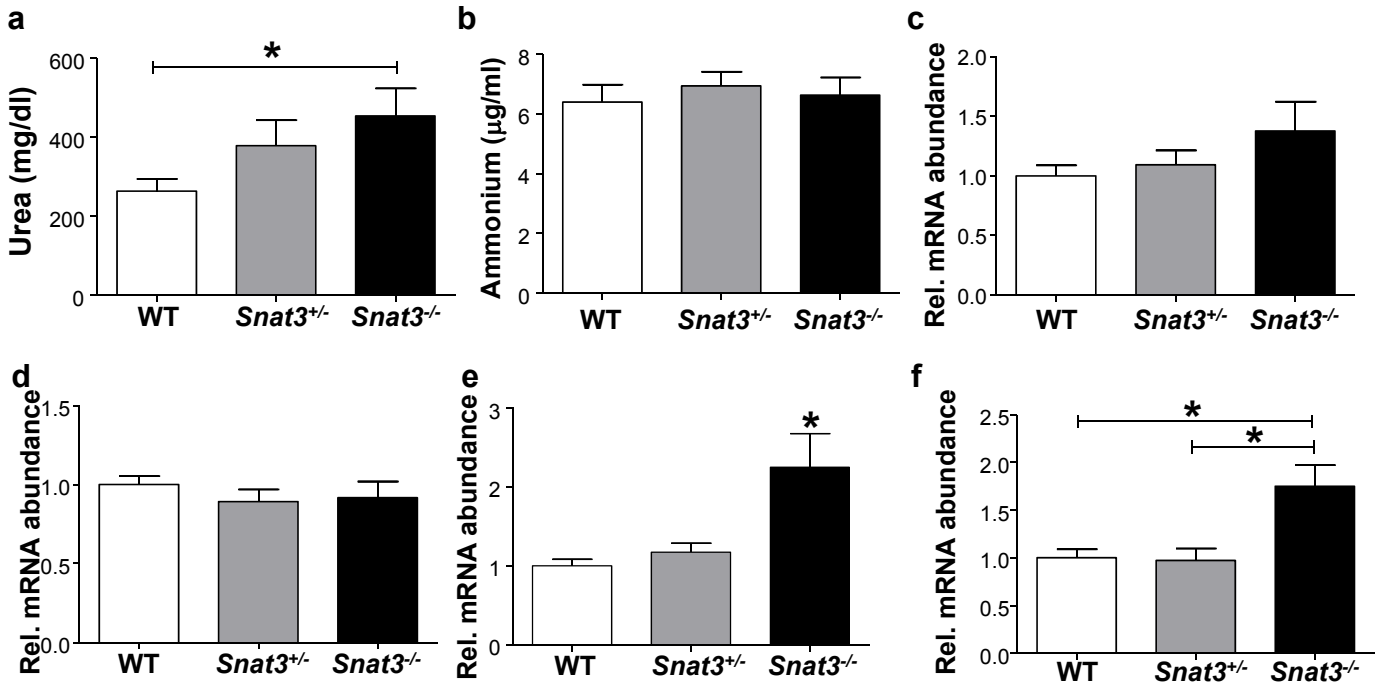
a
Urea (mg/dl)
600
400
200
0
*
WT
Snat3+/-
Snat3-/-
b
Ammonium (μg/ml)
8
6
4
2
0
WT
Snat3+/-
Snat3-/-
c
Rel. mRNA abundance
2.0
1.5
1.0
0.5
0.0
WT
Snat3+/-
Snat3-/-
d
Rel. mRNA abundance
1.5
1.0
0.5
0.0
WT
Snat3+/-
Snat3-/-
e
Rel. mRNA abundance
3
2
1
0
*
WT
Snat3+/-
Snat3-/-
f
Rel. mRNA abundance
2.5
2.0
1.5
1.0
0.5
0.0
*
*
WT
Snat3+/-
Snat3-/-

Fig6

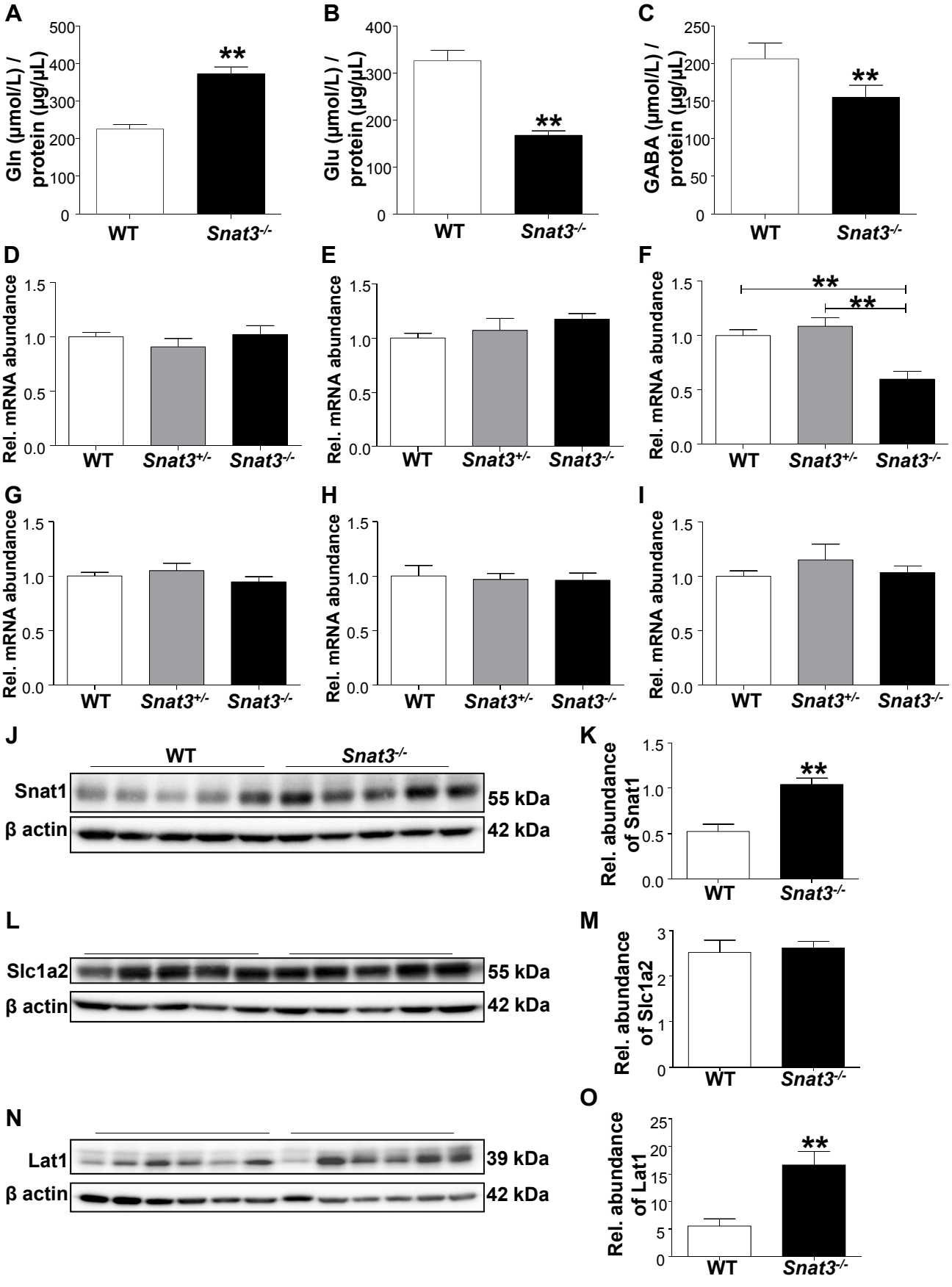
A
Gln (μmol/L) / protein (μg/μL)
500
400
300
200
100
0
**
WT
Snat3-/-
B
Glu (μmol/L) / protein (μg/μL)
400
300
200
100
0
**
WT
Snat3-/-
C
GABA (μmol/L) / protein (μg/μL)
250
200
150
100
50
0
**
WT
Snat3-/-
D
Rel. mRNA abundance
1.5
1.0
0.5
0.0
WT
Snat3+/-
Snat3-/-
E
Rel. mRNA abundance
1.5
1.0
0.5
0.0
WT
Snat3+/-
Snat3-/-
F
Rel. mRNA abundance
**
**
1.5
1.0
0.5
0.0
WT
Snat3+/-
Snat3-/-
G
Rel. mRNA abundance
1.5
1.0
0.5
0.0
WT
Snat3+/-
Snat3-/-
H
Rel. mRNA abundance
1.5
1.0
0.5
0.0
WT
Snat3+/-
Snat3-/-
I
Rel. mRNA abundance
1.5
1.0
0.5
0.0
WT
Snat3+/-
Snat3-/-
J
WT
Snat3-/-
Snat1
55 kDa
β actin
42 kDa
K
Rel. abundance of Snat1
1.5
1.0
0.5
0.0
**
WT
Snat3-/-
L
Slc1a2
55 kDa
β actin
42 kDa
M
Rel. abundance of Slc1a2
3
2
1
0
WT
Snat3-/-
N
Lat1
39 kDa
β actin
42 kDa
O
Rel. abundance of Lat1
25
20
15
10
5
0
**
WT
Snat3-/-

Fig7

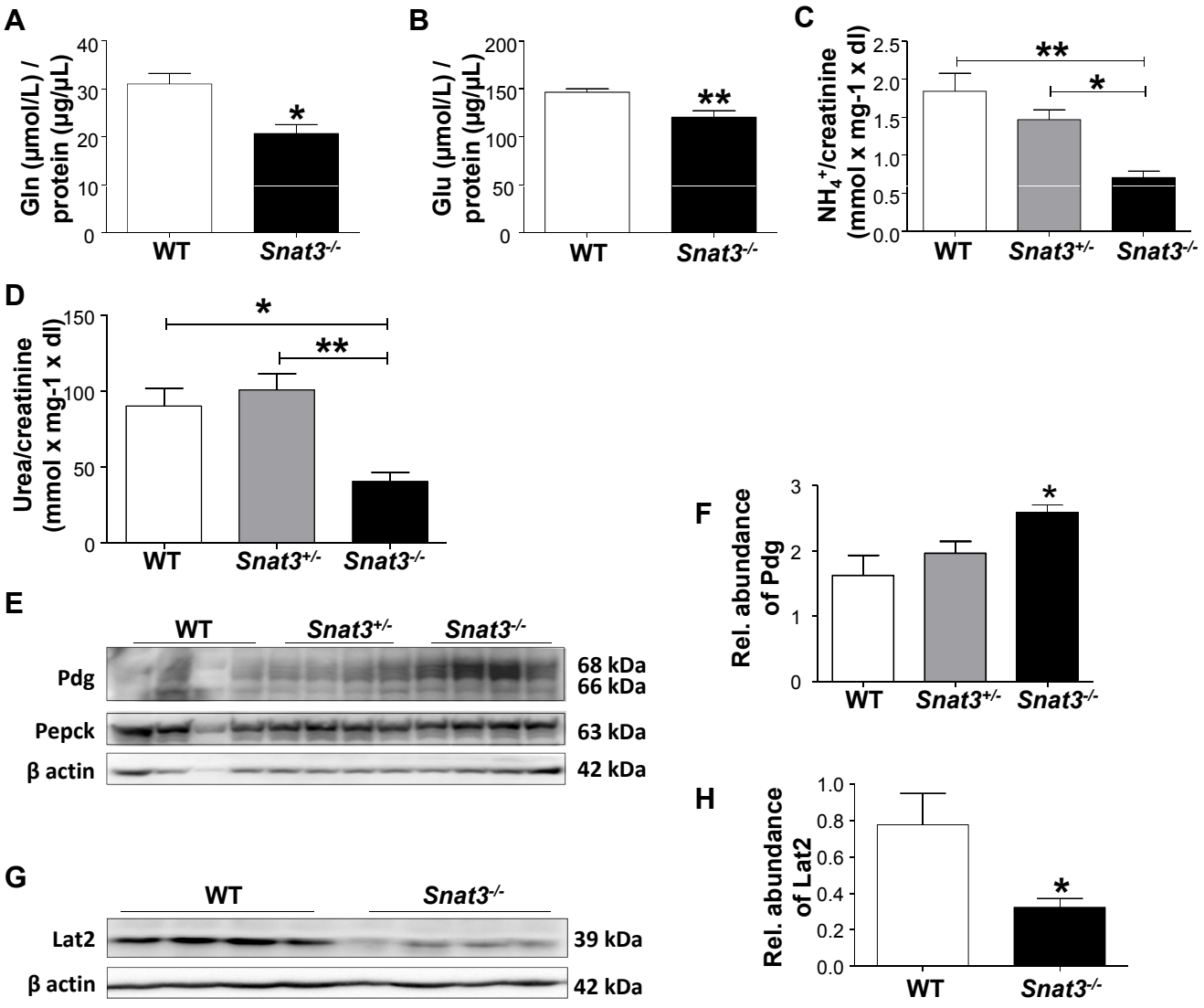
A
Gln (μmol/L) / protein (μg/μL)
40
30
20
10
0
*
WT
Snat3-/-
B
Glu (μmol/L) / protein (μg/μL)
200
150
100
50
0
**
WT
Snat3-/-
C
NH4+/creatinine (mmol x mg-1 x dl)
2.5
2.0
1.5
1.0
0.5
0.0
**
*
WT
Snat3+/-
Snat3-/-
D
Urea/creatinine (mmol x mg-1 x dl)
150
100
50
0
*
**
WT
Snat3+/-
Snat3-/-
E
WT
Snat3+/-
Snat3-/-
Pdg
68 kDa
66 kDa
Pepck
63 kDa
β actin
42 kDa
F
Rel. abundance of Pdg
3
2
1
0
*
WT
Snat3+/-
Snat3-/-
G
WT
Snat3-/-
Lat2
39 kDa
β actin
42 kDa
H
Rel. abundance of Lat2
1.0
0.8
0.6
0.4
0.2
0.0
*
WT
Snat3-/-

Fig8

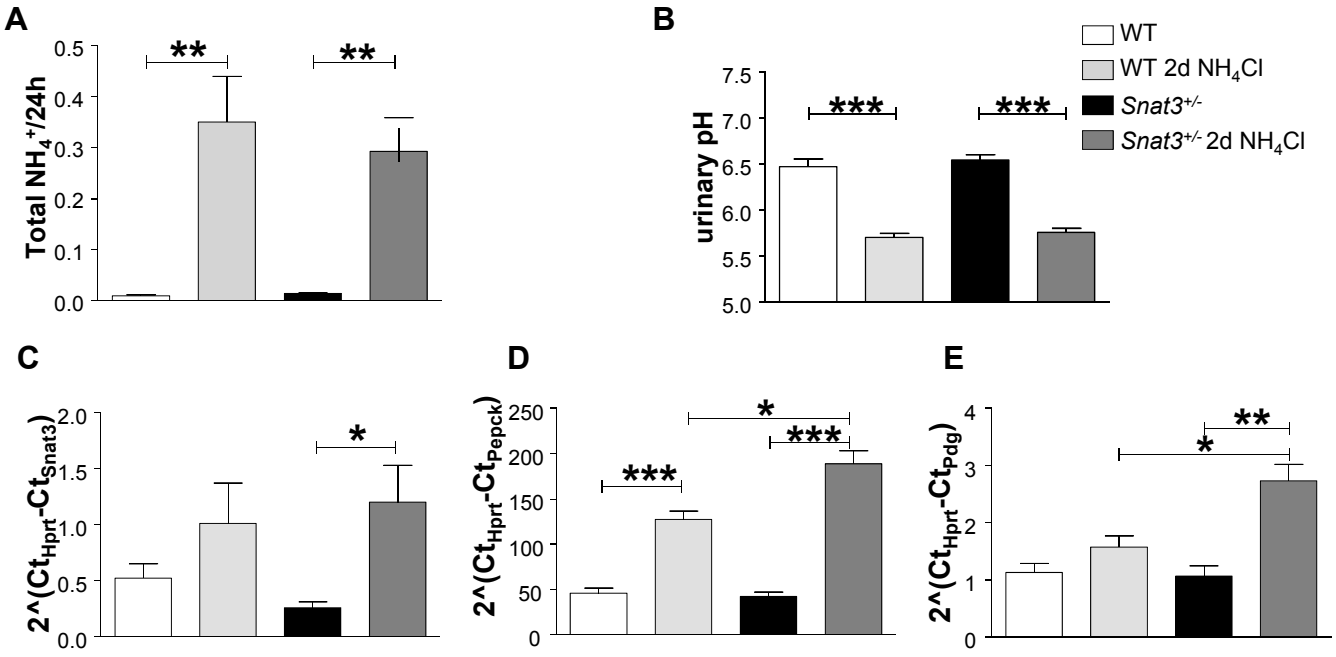
A
Total NH4+/24h
0.5
0.4
0.3
0.2
0.1
0.0
**
**
B
urinary pH
7.5
7.0
6.5
6.0
5.5
5.0
***
***
WT
WT 2d NH4Cl
Snat3+/-
Snat3+/- 2d NH4Cl
C
2^(CtHprt-CtSnat3)
2.0
1.5
1.0
0.5
0.0
*
D
2^(CtHprt-CtPepck)
250
200
150
100
50
0
*
***
***
E
2^(CtHprt-CtPdg)
4
3
2
1
0
**
*

Suppl. Figure 1 mRNA expresssion of selected genes in kidneys from in *Snat3*$^{-/-}$ compared to wild-type kidney samples (a-c) mRNA renal expression of the ammonia transporter *Rhcg* (Rhesus blood group family type C glycoprotein), the sodium-coupled neutral amino acid transporter 2 (*Snat2*) and 5 (*Snat5*) were measured by RT-qPCR in all mice, n = 10-13/genotype. *Rhcg* and *Snat2* showed no difference but *Snat5* was downregulated in kidneys from Snat3 deficient mice. *$P \leq 0.05$, **$P \leq 0.01$

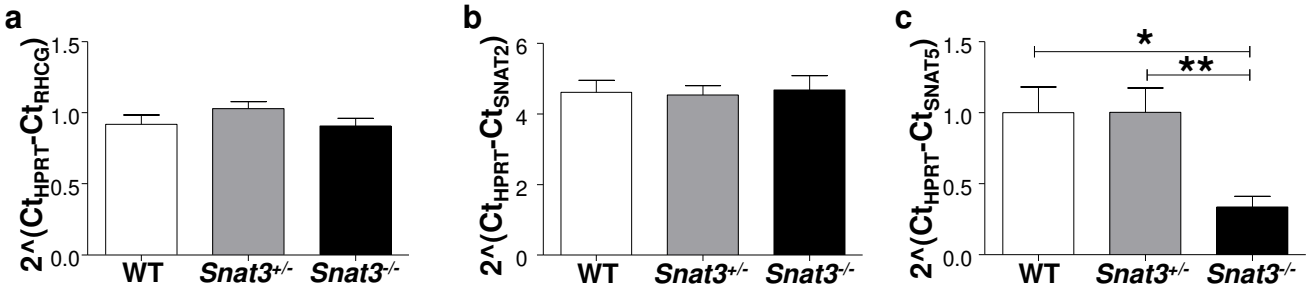

Supl. Table 1 Primers and probes

Gene	Acc. No.	Primers	Probes
ARG2(M)	AB047402	F: 5'- GCT CCA AGC CAA AGT CCT TAG A-3' (4-26) R: 5'-CCT CGA GGC TGT CCT TTT GA-3' (46-66)	5'-CCT CGA GGC TGT CCT TTT GA-3' (28-48)
ASL(M)	NM_133768	F: 5'-CCCAAGGCACCTTCAAATTA-3' (323-343) R: 5'-GCGACTTCGTCCTGTGTGTA-3' (438-458)	5'-GCCTGAAGGAACTCATCGGTGAAGC-3' (383-408)
ASS(M)	MUSASSA01	F: 5'-GGCCAGGAAAGCAGACTACA-3' (146-166) R: 5'-CACGAGGATGCAGGAGGT-3' (268-286)	5'-AAGGGCTCTGTGGTTCTGGCCTACA-3' (212-23.7)
CPS1(M)	NM_001080809	F: 5'-TGTCCGAGATGCAGATGATAAC-3' (1908-1930) R: 5'-ACATCTGGAACTCTGCATTGG-3' (2038-2059)	5'-CATGGGTGTTCACACAGGTGACTCG-3' (1965-1990)
GDH(M)	NM_008133	F: 5'-ACCATGTGTTGAGCCTCTCC-3' (338-358) R: 5'-GCCAGTGCTTTTACTTCATCC-3' (474-495)	5'-GGGAGGTATCCGTTACAGCA-3' (441-461)
GLU1(M)	NM_008131	F: 5'-CAAGTGTGTGGAAGAGTTACCTGAGT-3' (153-179) R: 5'-TGAAGGCTCCAACAGCGAC-3' (209-228)	5'-AACTTTGATGGCTCTAGTACCTTTCAG-3' (180-207)
HPRT(M)	NM_013556	F: 5'-TTATCAGACTGAAGAGCTACTGTAAGATC-3' (442-471) R: 5'-TTACCAGTGTCAATTATATCTTCAACAATC-3' (539-568)	5'-TGAGAGATCATCTCCACCAATAACTTTTATGTCCC-3' (481-515)
IGF1(M)	NM_010512	F: 5'-AGATCTGCCTCTGTGACTTCTTG-3' (38-61) R: 5'- CCTGTGGCCTTGTTGAAGTAA-3' (213-238)	5'-CACCTCTTCTACCTGGCGCTCTGCT-3' (90-111)
OTC(M)	NM_008769	F: 5'-AAATTCGGGATGCACCTTC-3' (628-647) R: 5'-GCTGCTTCCAGTGGATCATT-3' (761-781)	5'-GCAGAGCAGTATGCCAAGGAGAATGG-3' (697-723)
PEPCK(M)	NM_028994	F: 5'-GTGGGCGATGACATTGCC-3' (1062-1079) R: 5'-ACTGAGGTGCCAGGAGCAAC-3' (1143-1162)	5'-CCCAAGGCAACTTAAGGGCTATCAACCC-3' (1096-1123)
PDG(M)	XM_976581	F: 5'-ATGTGTTGGTCTCCTCTCTTGA-3' (1510-1532) R: 5'-TTGATCACCTCCTTCTCTCCG-3' (1642-1662)	5'-AGATGGGCAACAGTGTTAAGGGAATTCACT-3' (1535-1564)
RHCG(M)	NM_019799	F: 5'-GTTGAAGAAGCGCAAGAA-3' (245-265) R: 5'-CGAAGACCATTGCGTGTACA-3' (320-339)	5'-TTACTATCGCTACCCGAGCTTCCAG-3' (293-317)
SLC1A1(M)	NM_009199	F: 5'-TGTTTGACTGGCTCCTGGACC-3' (472-493) R: 3'-GCTCCAGCTCCTTCTTCGAGA-3' (1391-1412)	5'-ATGCGTTTGGGACGGGCA-3' (1361-1379)
SLC1A2(M)	NM_001077514	F: 5'-CCAGCAGATTGCAGACAGTGACAA-3' (555-579) R: 5'-CCGCCTTGGTGGTATTGG-3' (611-629)	5'-TGGTGGCACCTCCATCCGAGG-3' (587-608)
SNAT1(M)	NM_134086	F: 5'-CGCGTGCACACCAAAGTATG-3' (873-892) R: 5'-AGATTGGCAGGACGGACG-3' (956-973)	5'-TACCAACCATCGCCTTCGCGTTTG-3' (923-946)
SNAT2(M)	NM_175121	F: 5'-CGTCCATCTCCTCCTCAAGA-3' (732-752) R. 5'-CATTGGGGCTATGTCAAGCT-3' (871-891)	5'-GGCGTATGGTCTGGCTGGAAAGCTA-3' (798-823)
SNAT3(M)	NM_023805	F: 5'-CGAATCATGCCCACTGACAA-3' (1478-1497) R: 5'-AACCGCAGCGAAACAAAGG-3' (1531-1549)	5'-AGCCTGCAAGATCCACCCCTAAAATCCT-3' (1500-1527)
SNAT5(M)	NM_172479	F: 5'-CCCTCACTGTGCCTGTTGTG-3' (1037-1057) R: 5'-CTTGCTTGGAAAGAGCAGCTG-3' (1083-1104)	5'-CCCTATCCGCCGAGCCCTCCA-3' (1062-1083)

Supl. Table 2 Plasma amino acid concentration in *Snat3*$^{-/-}$ compared to wildtype mice

Amino acid	Wildtype (µmol/L)	*Snat3*$^{-/-}$ (µmol/L)
Alanine (Ala)	778.82 ± 45.07	541.17 ± 26.83***
Arginine (Arg)	196.45 ± 25.35	153.73 ± 12.64
Argininosuccinic acid (Asa)	n.d.	n.d.
Anserine (Ans)	n.d.	n.d.
Asparagine (Asn)	108.26 ± 6.65	120.13 ± 5.39
Aspartic acid (Asp)	28.59 ± 4.82	20.83 ± 2.51
α-Aminoadipic acid (Aad)	n.d.	n.d.
α-amino-n-butyric acid (Abu)	16.50 ± 3.12	20.27 ± 2.98
β-Aminoisobutyric (bAib)	n.d.	n.d.
Carnosine (Car)	9.88 ± 0.78	20.50 ± 3.03***
Citruline (Cit)	102.97 ± 4.15	103.67 ± 3.54
Cystathionine (Cth)	n.d.	n.d.
Cysteine (Cys)	3.05 ± 0.04	3.31 ± 0.20**
Ethanolamine (EtN)	31.11 ± 2.35	40.83 ± 8.05
GABA	n.d.	n.d.
Glutamate (Glu)	87.91 ± 10.75	**63.83** ± 7.57
Glutamine (Gln)	827.91 ± 43.67	831.25 ± 46.41
Glycine (Gly)	623.55 ± 32.83	676.08 ± 67.07
Histidine (His)	120.99 ± 12.09	469.36 ± 39.54***
Hydroxylysine (Hyl)	n.d.	n.d.
Hydroxyproline (Hyp)	88.75 ± 5.68	80.28 ± 9.51
Isoleucine (Ile)	95.07 ± 4.35	120.35 ± 14.40
Leucine (Leu)	133.36 ± 7.79	191.95 ± 26.84*
Lysine (Lys)	472.00 ± 34.97	424.50 ± 31.25
Methionine (Met)	92.20 ± 9.53	75.37 ± 5.40
o-Phosphoethanolamine (PEtN)	18.81 ± 0.09	13.88 ± 2.27
Ornithine (Orn)	152.09 ± 14.37	134.57 ± 12.20
Phenylalanine (Phe)	80.28 ± 4.05	86.02 ± 5.38
Proline (Pro)	309.09 ± 25.60	241.25 ± 19.09
Serine (Ser)	308.64 ± 20.50	39.25 ± 22.10
Taurine (Tau)	689.00 ± 77.36	608.67 ± 66.96
Threonine (Thr)	231.45 ± 26.81	293.92 ± 14.45*
Tryptophane (Trp)	87.70 ± 4.43	67.30 ± 6.01**
Tyrosine (Tyr)	150.32 ± 13.41	95.08 ± 9.47**
Valine (Val)	216.27 ± 10.31	266.25 ± 33.31

*P-value < 0.05, **P-value < 0.01, ***P-value < 0.001

Supl. Table 3 Liver amino acid content in *Snat3*$^{-/-}$ compared to wild-type mice

Amino acid	Wildtype (µmol.L^{-1}/µg protein.µL^{-1})	*Snat3*$^{-/-}$ (µmol.L^{-1}/µg protein.µL^{-1})
Alanine (Ala)	57.52 ± 9.72	28.99 ± 4.99 **
Arginine (Arg)	0.15 ± 0.01	0.14 ± 0.03
Argininosuccinic acid (Asa)	n.d.	n.d.
Anserine (Ans)	0.06 ± 0.04	0.02 ± 00 **
Asparagine (Asn)	3.67 ± 0.32	1.82 ± 0.24 **
Aspartic acid (Asp)	11.46 ± 3.49	10.46 ± 3.53
α-Aminoadipic acid (Aad)	1.18 ± 0.31	1.62 ± 0.24
α-Amino-n-butyric acid (Abu)	1.59 ± 0.15	2.28 ± 0.46
β-Aminoisobutyric (bAib)	1.81 ± 0.05	4.25 ± 0.68
Carnosine (Car)	0.24 ± 0.09	0.19 ± 0.03
Citruline (Cit)	1.17 ± 0.11	20.9 ± 0.36 *
Cystathionine (Cth)	0.43 ± 0.12	0.34 ± 0.06
Cysteine (Cys)	0.08 ± 0.02	0.06 ± 0.02
Ethanolamine (EtN)	2.05 ± 0.37	2.30 ± 0.88
GABA	0.58 ± 0.05	0.62 ± 0.09
Glutamate (Glu)	67.40 ± 6.96	42.88 ± 11.46 **
Glutamine (Gln)	84.02 ± 10.11	36.76 ± 7.63**
Glycine (Gly)	47.75 ± 5.74	45.20 ± 4.59
Histidine (His)	9.25 ± 0.74	8.32 ± 0.91
Hydroxylysine (Hyl)	n.d.	n.d.
Hydroxyproline (Hyp)	1.75 ± 0.15	15.68 ± 1.77 *
Isoleucine (Ile)	3.65 ± 0.31	2.17 ± 0.29 **
Leucine (Leu)	6.22 ± 0.57	4.26 ± 0.47
Lysine (Lys)	7.90 ± 0.88	7.75 ± 0.88
Methionine (Met)	0.53 ± 0.05	0.28 ± 0.06
o-Phosphoethanolamine (PEtN)	21.65 ± 1.60	16.95 ± 3.01
Ornithine (Orn)	8.07 ± 0.97	5.36 ± 1.07
Phenylalanine (Phe)	2.37 ± 0.28	1.20 ± 0.21 *
Proline (Pro)	9.09 ± 0.99	6.08 ± 0.94
Serine (Ser)	11.80 ± 1.16	15.68 ± 1.77
Taurine (Tau)	333.04 ± 40.88	172.74 ± 38.11 *
Threonine (Thr)	7.91 ± 0.48	9.60 ± 0.84 **
Tryptophane (Trp)	1.00 ± 0.09	0.50 ± 0.06
Tyrosine (Tyr)	2.88 ± 0.30	1.48 ± 0.18 **
Valine (Val)	5.96 ± 0.51	3.81 ± 0.49 *

* *P-value* < 0.05, ** *P-value* < 0.01, *** *P-value* < 0.001

Supl. Table 4 Brain amino acid content in *Snat3*$^{-/-}$ compared to wild-type mice

Amino acid	Wildtype (µmol.L^{-1}/µg protein.µL^{-1})	*Snat3*$^{-/-}$ (µmol.L^{-1}/µg protein.µL^{-1})
Alanine (Ala)	65.55 ± 4.18	40.02 ± 3.40 **
Arginine (Arg)	10.53 ± 0.62	9.23 ± 0.62
Argininosuccinic acid (Asa)	0.45 ± 0.09	0.43 ± 0.06
Anserine (Ans)	0.24 ± 0.03	0.35 ± 0.01 **
Asparagine (Asn)	8.07 ± 0.46	3.80 ± 0.31 **
Aspartic acid (Asp)	87.35 ± 10.04	34.02 ± 7.71 **
α-Aminoadipic acid (Aad)	0.74 ± 0.09	0.67 ± 0.07
α-Amino-n-butyric acid (Abu)	1.88 ± 0.13	1.31 ± 0.24
β-Aminoisobutyric (bAib)	1.02 ± 0.27	0.98 ± 0.19
Carnosine (Car)	3.0 ± 0.46	0.35 ± 0.01 **
Citruline (Cit)	2.33 ± 0.16	2.63 ± 0.16
Cystathionine (Cth)	4.36 ± 0.95	3.17 ± 0.47
Cysteine (Cys)	n.d.	n.d.
Ethanolamine (EtN)	13.61 ± 2.44	19.26 ± 4.20
GABA	206.45 ± 20.80	154.73 ± 16.49 **
Glutamate (Glu)	325.78 ± 22.12	167.15 ± 9.46 **
Glutamine (Gln)	225.13 ± 12.40	371.73 ± 19.36 **
Glycine (Gly)	107.44 ± 11.72	151.84 ± 1402
Histidine (His)	5.72 ± 0.52	14.26 ± 2.80 **
Hydroxylysine (Hyl)	n.d.	n.d.
Hydroxyproline (Hyp)	4.14 ± 0.47	3.57 ± 1.15
Isoleucine (Ile)	3.42 ± 0.33	2.20 ± 0.33 *
Leucine (Leu)	4.84 ± 0.59	3.58 ± 0.62 *
Lysine (Lys)	21.38 ± 1.34	36.37 ± 3.33 **
Methionine (Met)	4.28 ± 0.81	1.40 ± 0.19 **
o-Phosphoethanolamine (PEtN)	160.36 ± 6.44	216.52 ± 24.08
Ornithine (Orn)	1.27 ± 0.13	1.24 ± 0.09
Phenylalanine (Phe)	3.90 ± 0.36	2.39 ± 0.29 **
Proline (Pro)	9.15 ± 0.62	10.82 ± 1.14
Serine (Ser)	72.86 ± 2.80	57.80 ± 4.76 *
Taurine (Tau)	1205.68 ± 39.27	1527.71 ± 104.80 **
Threonine (Thr)	27.49 ± 3.16	18.86 ± 2.12
Tryptophane (Trp)	2.23 ± 0.14	1.06 ± 0.12 **
Tyrosine (Tyr)	7.08 ± 0.94	2.24 ± 0.23 **
Valine (Val)	6.90 ± 0.63	3.76 ± 0.58 **

* *P-value* < 0.05, ** *P-value* < 0.01, *** *P-value* < 0.001

Supl. Table 5 Kidney amino acid content in *Snat3*$^{-/-}$ compared to wild-type mice

Amino acid	Wildtype (µmol.L^{-1}/µg protein.µL^{-1})	*Snat3*$^{-/-}$ (µmol.L^{-1}/µg protein.µL^{-1})
Alanine (Ala)	43.13 ± 4.13	28.32 ± 3.34
Arginine (Arg)	5.60 ± 0.20	4.15 ± 0.25 **
Argininosuccinic acid (Asa)	0.46 ± 0.04	0.28 ± 0.03 **
Anserine (Ans)	0.05 ± 0.01	0.04 ± 00
Asparagine (Asn)	7.51 ± 0.74	6.17 ± 0.60
Aspartic acid (Asp)	41.95 ± 2.62	28.33 ± 1.81 **
α-Aminoadipic acid (Aad)	1.55 ± 0.07	1.26 ± 0.17
α-amino-n-butyric acid (Abu)	1.45 ± 0.13	3.10 ± 0.92 *
β-Aminoisobutyric (bAib)	1.11 ± 0.05	1.84 ± 0.29 **
Carnosine (Car)	0.45 ± 0.04	0.4 ± 0.07
Citruline (Cit)	1.64 ± .014	1.68 ± 0.16
Cystathionine (Cth)	0.25 ± 0.03	0.17 ± 0.01 *
Cysteine (Cys)	80.6 ± 0.25	8.30 ± 0.80
Ethanolamine (EtN)	11.81 ± 0.75	17.44 ± 2.50
GABA	1.42 ± 0.13	1.31 ± 0.09
Glutamate (Glu)	146.70 ± 3.43	120.34 ± 6.86 **
Glutamine (Gln)	30.76 ± 2.68	23.29 ± 2.89 *
Glycine (Gly)	152.27 ± 7.52	171.19 ± 18.20
Histidine (His)	3.79 ± 0.38	12.28 ± 2.39 **
Hydroxylysine (Hyl)	0.26 ± 0.02	0.15 ± 0.02 **
Hydroxyproline (Hyp)	14.72 ± 1.30	6.95 ± 2.08 *
Isoleucine (Ile)	4.56 ± 0.25	4.00 ± 0.12
Leucine (Leu)	7.82 ± 0.51	7.56 ± 0.32
Lysine (Lys)	9.12 ± 0.37	8.42 ± 0.93
Methionine (Met)	1.71 ± 0.11	1.07 ± 0.19 **
o-Phosphoethanolamine (PEtN)	79.98 ± 2.81	90.12 ± 5.15
Ornithine (Orn)	2.12 ± 0.09	1.57 ± 0.13 **
Phenylalanine (Phe)	3.24 ± 0.15	3.12 ± 0.20
Proline (Pro)	18.35 ± 1.95	12.36 ± 1.26
Serine (Ser)	25.93 ± 2.04	22.48 ± 2.89
Taurine (Tau)	337.52 ± 11.63	348.49 ± 35.33
Threonine (Thr)	15.05 ± 1.12	16.08 ± 2.23
Tryptophane (Trp)	1.64 ± 0.02	1.18 ± 0.09 **
Tyrosine (Tyr)	5.34 ± 0.61	2.92 ± 0.24 **
Valine (Val)	9.00 ± 0.45	7.81 ± 0.31

* *P-value* < 0.05, ** *P-value* < 0.01, *** *P-value* < 0.001